SCORE: Spurious COrrelation REduction for Offline Reinforcement Learning

Zhihong Deng[*]
University of Technology Syndey

Zuyue Fu
Northwestern University

Lingxiao Wang
Northwestern University

Zhuoran Yang
Princeton University

Chenjia Bai
Harbin Institute of Technology

Zhaoran Wang
Northwestern University

Jing Jiang
University of Technology Syndey

Abstract

Offline reinforcement learning (RL) aims to learn the optimal policy from a pre-collected dataset without online interactions. Most of the existing studies focus on distributional shift caused by out-of-distribution actions. However, even in-distribution actions can raise serious problems. Since the dataset only contains limited information about the underlying model, offline RL is vulnerable to spurious correlations, i.e., the agent tends to prefer actions that by chance lead to high returns, resulting in a highly suboptimal policy. To address such a challenge, we propose a practical and theoretically guaranteed algorithm SCORE that reduces spurious correlations by combing an uncertainty penalty into policy evaluation. We show that this is consistent with the pessimism principle studied in theory, and the proposed algorithm converges to the optimal policy with a sublinear rate under mild assumptions. By conducting extensive experiments on existing benchmarks, we show that SCORE not only benefits from a solid theory but also obtains strong empirical results on a variety of tasks.

1 Introduction

In offline reinforcement learning (RL), agents learn from a static dataset without any interaction with the environment. Although off-policy RL algorithms are intuitively applicable to this setting, they often perform poorly in practice [Fujimoto et al., 2019, Fu et al., 2020]. Many research works attribute this problem to distributional shift [Fujimoto et al., 2019, Wu et al., 2019, Levine et al., 2020], especially *action* distributional shift. The out-of-distribution (OOD) actions used in Bellman backups introduce extrapolation errors in the value function and the agent fails to correct such errors since no online interaction is allowed. However, in-distribution actions also raise significant challenges. When the dataset has insufficient information about the underlying Markov Decision Process (MDP), suboptimal actions with high uncertainty in knowledge may appear to be good and thus bias the agent towards making bad decisions. In other words, epistemic uncertainty spuriously correlates with decision-making.

In this paper, we assume that an effective mechanism to deal with spurious correlations is the key ingredient missing in existing methods. Recently, some theoretical studies found that pessimism in the face of uncertainty eliminates spurious correlations in offline learning [Jin et al., 2021, Xie et al., 2021]. Furthermore, the pessimism principle is provably efficient and even achieves mini-max optimal in linear MDPs [Jin et al., 2021]. However, it is empirically shown to fail when combining with function approximators, e.g., neural networks, to solve general MDPs. The two major difficulties come from quantifying uncertainty [Levine et al., 2020, Yu et al., 2021] and constraining the action space [Fujimoto et al., 2019].

To address these problems, we design a practical algorithm termed Spurious COrrelation REduction (SCORE), which adds an uncertainty penalty into value estimators, i.e., the higher the uncertainty the more the action value will be penalized. In this way, the spurious correlation between epistemic uncertainty and decision-making is alleviated. Implementation-wise, we use bootstrapped ensemble Q networks to quantify the uncertainty. Meanwhile, a gradually

[*] Correspondence to: Zhihong Deng (zhi-hong.deng@student.uts.edu.au).

decaying behavior cloning (BC) regularizer is added into the policy objective to constrain the action space. Accordingly, the proposed method reduces to a pure uncertainty-based method when the regularization coefficient decreases to zero, avoiding the dependence on the behavioral policy. We further show that this method is theoretically guaranteed and achieves a sublinear rate of convergence under linear function approximation. Some previous papers constrain the action space by enforcing a strong constraints between the learned policy and the behavioral policy [Fujimoto et al., 2019, Wu et al., 2019, Kumar et al., 2019] or regularizing the action value [Kumar et al., 2020]. While these methods show good empirical results for particular data distributions, the performance is closely related to the behavioral policy. In contrast, our approach is theoretically adaptive to the data distribution, and the performance depends only on how well the dataset covers the state-action distribution of the optimal policy, rather than the entire state-action space [Jin et al., 2021].

Our main contributions are as follows: (1) We demonstrate the detrimental effect of spurious correlations in offline RL and show that pessimism in the face of uncertainty can eliminate it, recovering the optimal policy. (2) We propose a practical algorithm that reduces spurious correlations with an uncertainty penalty estimated by bootstrapped ensemble Q networks. We prove that this is in line with the pessimism principle from the Bayesian perspective. (3) We also show that the proposed method converges to the optimal policy with a sublinear rate under linear function approximation. (4) Through extensive experiments on the D4RL benchmark, we show that SCORE is robust across multiple data settings, which indicates that the pessimism principle in offline RL is not only theoretically sound but also strongly supported by empirical results.

2 Preliminaries

We consider an MDP $\mathcal{M} = (\mathcal{S}, \mathcal{A}, P, R, \gamma, d_0)$, where $\mathcal{S}$ and $\mathcal{A}$ represent the state space and the action space respectively. $P\colon \mathcal{S} \times \mathcal{S} \times \mathcal{A} \to [0,1]$ is the Markov transition function, $R\colon \mathcal{S} \times \mathcal{A} \to \mathbb{R}$ is the reward function, $\gamma \in (0,1)$ is the discount factor, and $d_0\colon \mathcal{S} \to [0,1]$ is the initial distribution of states.

In offline RL, the agent is given a static dataset $\mathcal{D} = \{(s_i, a_i, s_i', r_i)\}_{i=1}^N$ collected by the behavioral policy π_β. Suppose that $d^\pi(s,a)$ denotes the discounted state-action distribution of a policy π, we have $(s_i, a_i) \sim d^{\pi_\beta}(\cdot,\cdot)$, $s_i' \sim P(\cdot \mid s_i, a_i)$ and $r_i = R(s_i, a_i)$. Then the goal of offline RL is to search for a policy $\pi\colon \mathcal{A} \times \mathcal{S} \to [0,1]$ that maximizes the expected total reward $\mathcal{J}(\pi) = \mathbb{E}_\pi[\sum_{t=0}^\infty \gamma^t \cdot R(\tilde{s}_t, \tilde{a}_t)]$ given a static dataset $\mathcal{D}$. The expectation $\mathbb{E}_\pi[\cdot]$ is taken with respect to $\tilde{s}_0 \sim d_0(\cdot)$, $\tilde{a}_t \sim \pi(\cdot \mid \tilde{s}_t)$, and $\tilde{s}_{t+1} \sim P(\cdot \mid \tilde{s}_t, \tilde{a}_t)$. With a slight abuse of notation, we refer to $\mathcal{D}$ as the dataset distribution.

2.1 Suboptimality Decomposition

In offline RL, the samples are drawn from a fixed distribution $\mathcal{D}$ instead of the environment. Therefore, the true Bellman optimality operator $\mathcal{B}$ gets replaced by its empirical counterpart $\widehat{\mathcal{B}}$ [2]. Since the dataset only covers partial information of the environment, the agent would be learning with bias. In this paper, we formalize such bias for any action-value function $Q\colon \mathcal{S} \times \mathcal{A} \to \mathbb{R}$ as follows:

$$\iota(s,a) = \mathcal{B}Q(s,a) - \widehat{\mathcal{B}}Q(s,a). \tag{1}$$

Since $\iota(s,a)$ characterizes the error arising from insufficient information about the environment in knowledge and gradually converges to zero as we learn more about the state-action pair (s,a) (including state transitions and rewards), we refer to it as the *epistemic error*. In the ideal case, the dataset accurately mirrors the environment, i.e., $\widehat{\mathcal{B}} = \mathcal{B}$, resulting in zero epistemic error. The agent can learn the optimal policy offline just like in the online setting. However, this is almost impossible in real-world domains. In general, the dataset contains limited information and the epistemic error persists throughout the learning process.

We decompose the suboptimality of a policy $\widehat{\pi}$, i.e., the performance gap between $\widehat{\pi}$ and the optimal policy π^*, into the following three components [Jin et al., 2021]:

$$\begin{aligned}&\operatorname{SubOpt}(\widehat{\pi}; s_0) = V^{\pi^*}(s_0) - V^{\widehat{\pi}}(s_0)\\ &= \underbrace{-\sum_{t=0}^\infty \gamma^t \mathbb{E}_{\widehat{\pi}}\left[\iota(s_t,a_t) \mid s_0\right]}_{\text{(i): Spurious Correlation}} + \underbrace{\sum_{t=0}^\infty \gamma^t \mathbb{E}_{\pi^*}\left[\iota(s_t,a_t) \mid s_0\right]}_{\text{(ii): Intrinsic Uncertainty}} + \underbrace{\sum_{t=0}^\infty \gamma^t \mathbb{E}_{\pi^*}\left[\left\langle \widehat{Q}\left(s_t,\cdot\right), \pi^*\left(\cdot \mid s_t\right) - \widehat{\pi}\left(\cdot \mid s_t\right)\right\rangle_{\mathcal{A}} \mid s_0\right]}_{\text{(iii): Optimization Error}},\end{aligned} \tag{2}$$

where $\widehat{Q}$ is an estimated Q function, $V^\pi(s) = \langle Q^\pi(s,\cdot), \pi(\cdot \mid s)\rangle$ is the state-value of a state s, and $V^\pi(s_0)$ measures the expected return of a policy π at the initial state s_0. It is straightforward that the suboptimality of the optimal policy

[2] In the empirical Bellman operator $\widehat{\mathcal{B}}$, transition probabilities and rewards are estimated by the sample average in $\mathcal{D}$.

π^* is zero and a lower suboptimality indicates a better policy. In linear MDPs, term (ii) in equation 2 arises from the information-theoretic lower bound and thus is impossible to eliminate. Meanwhile, term (iii) is non-positive as long as the policy $\widehat{\pi}$ is greedy with respect to the estimated action-value function $\widehat{Q}$. Therefore, controlling term (i) is the key to reduce suboptimality in offline RL. We accomplish this by introducing pessimism in the following sections.

2.2 Pessimism

Let $\widehat{Q}\colon \mathcal{S} \times \mathcal{A} \to \mathbb{R}$ represents an arbitrary estimated Q-value function. We first define an uncertainty quantifier U with confidence $\xi \in (0,1)$ as follows.

Definition 2.1 (ξ-Uncertainty Quantifier)**.** $U : \mathcal{S} \times \mathcal{A} \to \mathbb{R}$ is a ξ-uncertainty quantifier with respect to the dataset distribution $\mathcal{D}$ if the event

$$\mathcal{E} = \left\{ |\widehat{\mathcal{B}}\widehat{Q}(s,a) - \mathcal{B}\widehat{Q}(s,a)| \le U(s,a) \text{ for all } (s,a) \in \mathcal{S} \times \mathcal{A} \right\} \tag{3}$$

satisfies $\Pr(\mathcal{E}|\mathcal{D}) \ge 1 - \xi$.

In Definition 2.1, U measures the uncertainty arising from approximating $\mathcal{B}\widehat{Q}$ with $\widehat{\mathcal{B}}\widehat{Q}$, where $\mathcal{B}$ is the true Bellman optimality operator while $\widehat{\mathcal{B}}$ is the empirical Bellman operator. We remark that $\widehat{\mathcal{B}}$ can be constructed implicitly by treating $\widehat{\mathcal{B}}\widehat{Q}\colon \mathcal{S} \times \mathcal{A} \to \mathbb{R}$ as a whole. When $\mathcal{B}\widehat{Q}$ and $\widehat{\mathcal{B}}\widehat{Q}$ differ by a large amount, U should be large, while when the two quantities are sufficiently close, U can be very small or even zero. We then construct a pessimistic Bellman operator as follows:

$$\widehat{\mathcal{B}}^{-}\widehat{Q}(s,a) := \widehat{\mathcal{B}}\widehat{Q}(s,a) - U(s,a). \tag{4}$$

According to Definition 2.1, $\widehat{\mathcal{B}}^{-}\widehat{Q}(s,a) \le \mathcal{B}\widehat{Q}(s,a)$ holds for all state-action pairs with a high probability, i.e., the Q-value obtained by equation 4 lower bounds the true value. In other words, equation 4 provides a pessimistic estimation of the Q function. Replacing the empirical Bellman operator $\widehat{\mathcal{B}}$ in equation 1 with the pessimistic Bellman operator, it holds that:

$$\iota(s,a) = \mathcal{B}\widehat{Q}(s,a) - \widehat{\mathcal{B}}^{-}\widehat{Q}(s,a) \begin{cases} \ge \mathcal{B}\widehat{Q}(s,a) - \widehat{\mathcal{B}}\widehat{Q}(s,a) + |\mathcal{B}\widehat{Q}(s,a) - \widehat{\mathcal{B}}\widehat{Q}(s,a)| \ge 0, \\ = \mathcal{B}\widehat{Q}(s,a) - \widehat{\mathcal{B}}\widehat{Q}(s,a) + U(s,a) \le 2U(s,a). \end{cases} \tag{5}$$

Since the epistemic error $\iota(s,a)$ is non-negative as shown in equation 5, term (i) in equation 2 only reduces the suboptimality. As a result, pessimism eliminates spurious correlations. In the meanwhile, the suboptimality is now upper-bounded by $\sum_{t=0}^{\infty} 2\gamma^t \mathbb{E}_{\pi^*}\left[U(s,a) \,|\, s_0\right]$, so what remains is to find a sufficiently small ξ-uncertainty quantifier to tighten this upper bound.

3 Spurious COrrelation REduction for Offline RL

In this section, we elaborate the method we used to reduce the impact of spurious correlations on the offline RL problem. We first demonstrate the spurious correlation phenomenon through a simple example in Section 3.1 and verify the effectiveness of the pessimistic Bellman operator. We then present a general algorithm named SCORE in Section 3.2. In Section 3.3, we further analyze the convergence of the proposed algorithm.

3.1 An Example of The Spurious Correlation Phenomenon

We consider an episodic MDP with two states $\mathcal{S} = \{s_{\text{good}}, s_{\text{bad}}\}$ and two actions $\mathcal{A} = \{a_{\text{good}}, a_{\text{bad}}\}$. We assume for any current state $s \in \mathcal{S}$ that $P(s_{\text{good}} \,|\, s, a_{\text{good}}) = 2/3$, $P(s_{\text{bad}} \,|\, s, a_{\text{good}}) = 1/3$, $P(s_{\text{good}} \,|\, s, a_{\text{bad}}) = 1/3$, and $P(s_{\text{bad}} \,|\, s, a_{\text{bad}}) = 2/3$. In s_{good}, the reward is always positive regardless of the action performed, while in the bad state s_{bad}, the agent can only get punished. As a result, it is optimal to always perform a_{good} to stay in/move to s_{good}. To demonstrate the effect of spurious correlations, we generate an expert dataset with the optimal policy and modify it by adding a trajectory starting from performing the bad action and transiting into the good state.

Figures 1(a) and 1(b) show the empirical transition probabilistic distribution of the two datasets. Since the optimal policy always prefers a_{good}, the empirical probabilities for a_{bad} are all zero. But in the modified dataset, $(s_{\text{good}}, a_{\text{bad}})$ appears once and transits into s_{good}, so the corresponding probability becomes one (the blue bar in Figure 1(b)). In this case, no OOD actions (both a_{good} and a_{bad} are included in the dataset) exist, but $(s_{\text{good}}, a_{\text{bad}})$ carries high uncertainty in knowledge. We run offline Q-learning and its pessimistic variant (equation 4) on the modified dataset. Figures 1(c) and 1(d) show how the Q values evolve during the training process. Since epistemic uncertainty spuriously correlates with decision-making, offline Q-learning overestimates $Q(s_{\text{good}}, a_{\text{bad}})$ and converges to a suboptimal policy favoring

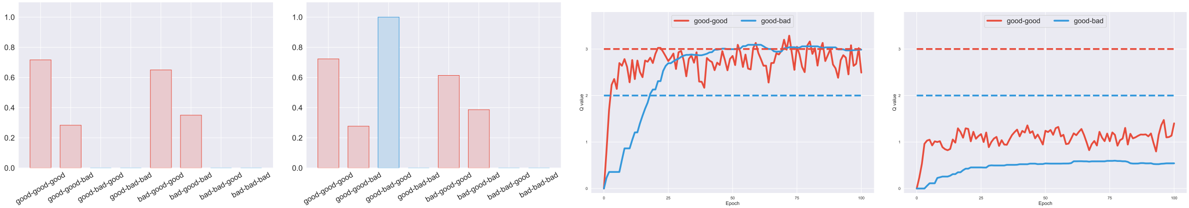

(a) (b) (c) (d)

Figure 1: (a) and (b) present the empirical transition probabilistic distribution of the expert dataset and the modified dataset respectively. The horizontal coordinates are in the form of "state-action-next_state", e.g., "good-bad-good" corresponds to the transition probability of transitioning to a good state after performing a bad action in a good state. (c) and (d) present the changes in Q value of performing different actions in the initial good state, with the former is learned by offline Q-learning and the latter is learned using equation 4. The horizontal dashed lines show the true Q values of performing the good action (blue) and the bad action (blue).

a_{bad}. By contrast, the pessimistic variant penalizes $Q(s_{\text{good}}, a_{\text{bad}})$ by high uncertainty, recovering the optimal policy, i.e., always prefers a_{good}. While most existing works focus on defending OOD actions, in this simple example, we show that even in-distribution data cause serious problems. Therefore, reducing spurious correlations is of significance in offline RL. We refer to Appendix D for more details about the example.

3.2 Practical Algorithms

As shown in Section 2.2 and the above example, pessimism can eliminate spurious correlations in offline RL. What remains is to design a proper uncertainty quantifier. From Definition 2.1 and equation 5, we can see that $U(s, a) = |\widehat{\mathcal{B}}\widehat{Q}(s, a) - \mathcal{B}\widehat{Q}(s, a)|$ achieves the tightest bound, i.e., the uncertainty quantifier U accurately measures the epistemic error ι. In other words, to eliminate spurious correlations, we need a method to provide reliable estimations of epistemic uncertainty. Since the state and the action space are huge in real-world domains, function approximation (e.g., use deep neural networks) is indispensable to provide sufficient expressiveness. In this case, we can neither directly estimate uncertainty by counting states and actions, nor derive an analytical form of the epistemic uncertainty as in linear MDPs [Jin et al., 2021].

Estimating uncertainty is an important research topic. One of the most popular approaches is to use the bootstrapped ensemble method [Osband et al., 2016, Lakshminarayanan et al., 2017]. Each ensemble member is trained on a different version of data generated by a bootstrap sampling procedure. This approach provides a general and non-parametric way to approximate the Bayesian posterior distribution, so the standard deviation of multiple Q estimations can be regarded as a reasonable estimation of the epistemic uncertainty. We remark that previous works mainly use uncertainty as a bonus in online RL to promote efficient exploration. In this paper, we utilize uncertainty as a penalty to reduce spurious correlations. For the equivalence of the uncertainty obtained by this method to the one studied in theory [Jin et al., 2021], we refer to Appendix C for more details.

Policy Evaluation. In the policy evaluation step, we maintain M independent critics $\{Q_{\theta_i}\}_{i=1}^{M}$ and their corresponding target networks $\{Q_{\theta_i'}\}_{i=1}^{M}$. The learning objective of each critic Q_{θ_i} is as follows,

$$\begin{aligned} \mathcal{L}(Q_{\theta_i}) &= \mathbb{E}_{s,a,s' \sim \mathcal{D}, a' \sim \pi(\cdot \mid s')} \left[\left(Q_{\theta_i}(s, a) - y_i \right)^2 \right], \\ y_i &= r + \gamma \left(Q_{\theta_i'}(s', a') - \beta u(s', a') \right) - \beta u(s, a). \end{aligned} \tag{6}$$

where $u(\cdot, \cdot)$ is the standard deviation of the M predictions of the input state-action pair, and β is a hyper-parameter that controls the strength of the uncertainty penalty. At first glance, there are two penalty terms in equation 6, one for the state-action pair (s, a) and the other for (s', a'), which is different from equation 4 used in PEVI [Jin et al., 2021]. The major reason is that PEVI is an algorithm for episodic MDPs, which calculates the Q values in one pass in an episodic backward manner starting from the terminal state. The target value it uses at step t has already been penalized at step $t + 1$, so subtracting $u(s', a')$ at step t is unnecessary. Conversely, we study non-episodic MDPs and the Q networks are optimized with stochastic gradient descent. Each sample is used multiple times in varying order, so it is more appropriate to penalize both (s, a) and (s', a') with a small quantity (controlled by β) each time. Empirically, the penalty term $u(s', a')$ is more effective than $u(s, a)$ since it also serves to defend against OOD actions. While the majority of existing approaches use the smallest Q-value as the target value to avoid overestimation, equation 6 updates each critic Q_{θ_i} towards its corresponding target network $Q_{\theta_i'}$. By doing so, the temporal consistency is guaranteed and the uncertainty can be passed over time [Osband et al., 2016, 2018].

Algorithm 1 Spurious COrrelation REduction (SCORE) for Offline RL

```
Initialize critic networks $\{Q_{\theta_i}\}_{i=1}^M$ and actor network $\pi_\phi$, with random parameters $\{\theta_i\}_{i=1}^M, \phi$
Initialize target networks $\{\theta_i'\}_{i=1}^M \leftarrow \{\theta_i\}_{i=1}^M, \phi' \leftarrow \phi$
Initialize replay buffer with the dataset $\mathcal{D}$
for $t = 1$ to $T$ do
    Sample a mini-batch of $n$ transitions $(s, a, s', r)$ from $\mathcal{D}$
    $a' \leftarrow \pi_{\phi'}(s') + \epsilon, \epsilon \sim \text{clip}(\mathcal{N}(0, \sigma^2), -c, c)$
    for $i = 1$ to $M$ do
        Update $\theta_i$ to minimize equation 6.                                ▷ Pessimism
    end for
    if $t\%d = 0$ then                                                 ▷ Delayed Policy Updates
        Update $\phi$ to maximize equation 7.
        Update target networks: $\theta_i' \leftarrow \tau\theta_i' + (1-\tau)\theta_i,\ \phi' \leftarrow \tau\phi' + (1-\tau)\phi$.
    end if
    if $t\%d_{\text{bc}} = 0$ then
        $\lambda = \gamma_{\text{bc}} \cdot \lambda$
    end if
end for
```

Policy Improvement. The objective function of the policy π_ϕ is defined as follows,

$$\mathcal{L}(\pi_\phi) = \mathbb{E}_{s,a\sim\mathcal{D}}\left[\min_i Q_{\theta_i}(s, \pi_\phi(s)) - \lambda\|\pi_\phi(s) - a\|_2^2\right], \tag{7}$$

The behavior cloning loss $\|\pi_\phi(s) - a\|_2^2$ serves as a regularization term, which frees the algorithm from explicitly modeling the behavioral policy π_β [Fujimoto et al., 2019, Kumar et al., 2019, Wu et al., 2021]. In particular, we gradually decrease the regularization coefficients λ during the training process. At the early stage, the ensemble networks are not accurate enough to measure epistemic uncertainty. The behavior cloning regularization helps to provide a good initialization and avoid the policy from deviating far away from the dataset distribution $\mathcal{D}$. In the later stage, the regularization effect becomes weaker and weaker, and the pessimistic Q-values gradually dominate the policy objective. In this way, SCORE returns to a pure uncertainty-based method without relying on the behavioral policy that generates the dataset. Alternatively, we can understand this design choice from the optimization perspective [Guo et al., 2020]. Directly maximizing the uncertainty-penalized value function is a difficult task. Using behavior cloning lowers the difficulty of the optimization problem at the early stage. As the training process proceeds, the regularization effect decreases, and the objective function gradually returns to the original problem, i.e., maximizing the pessimistic action-value function. The complete algorithm is summarized in Algorithm 1.

3.3 Convergence Analysis

In this section, we first introduce offline soft-DPG, which is the theoretical counterpart of SCORE. Then we show the equivalence between offline soft-DPG and offline proximal policy optimization (PPO, Schulman et al. [2015, 2017]). Finally, by analyzing the convergence of offline PPO, we show that offline soft-DPG achieves a sublinear rate of convergence.

Regularized MDP. For any behavior policy π_0, based on the definition of the MDP $\mathcal{M} = (\mathcal{S}, \mathcal{A}, P, R, \gamma, d_0)$, we introduce its regularized counterpart $\mathcal{M}_\lambda = (\mathcal{S}, \mathcal{A}, P, R, \gamma, d_0, \lambda)$, where λ is the regularization parameter. Specifically, for any policy π in $\mathcal{M}_\lambda$, the regularized state-value function V_λ^π and the regularized action-value function Q_λ^π are defined as

$$\begin{aligned} V_\lambda^\pi(s) &= \mathbb{E}_\pi\left[\sum_{t=0}^\infty \gamma^t \cdot \big(r(s_t, a_t) - \lambda \cdot \log\big(\pi(\cdot\,|\,s_t)/\pi_0(\cdot\,|\,s_t)\big)\big)\,\Big|\, s_0 = s\right], \\ Q_\lambda^\pi(s, a) &= r(s, a) + \gamma \cdot \mathbb{E}_{s'\sim P(\cdot\,|\,s,a)}\big[V_\lambda^\pi(s')\big], \qquad \text{for any } (s, a) \in \mathcal{S} \times \mathcal{A}, \end{aligned}$$

respectively. We remark that such a regularization term in the definition of V_λ^π serves as a behavior cloning term. Throughout the learning process, we anneal the regularization parameter λ so that the impact of the behavior cloning term decreases. Formally, for a collection of regularized MDPs $\{\mathcal{M}_{\lambda_k}\}_{k=0}^K$, we aim to minimize the suboptimality gap defined as follows,

$$\text{SubOptGap}(K) = \min_{k\in\{0,1,\ldots,K-1\}} \big(V_k^*(s_0) - V_k^{\pi_k}(s_0)\big). \tag{8}$$

Here we denote by $V_k^* = V_{\lambda_k}^{\pi_k^*}$ and $V_k^{\pi_k} = V_{\lambda_k}^{\pi_k}$ for notational convenience, where $\pi_k^* \in \arg\max_\pi \mathbb{E}_{s_0 \sim d_0}[V_{\lambda_k}^{\pi}(s_0)]$ is the optimal policy for $\mathcal{M}_{\lambda_k}$. We remark that the suboptimality defined in equation 8 measures the suboptimality gap between the best policy π_{k^*} and the corresponding optimal policy $\pi_{k^*}^*$ under the regularized MDP $\mathcal{M}_{\lambda_{k^*}}$, where $k^* = \arg\min_{k \in \{0,1,\ldots,K-1\}}(V_k^*(s_0) - V_k^{\pi_k}(s_0))$.

Pessimistic Offline Soft-DPG. For the simplicity of presentation, we consider a theoretical counterpart of the proposed algorithm. Formally, we introduce pessimistic offline soft-DPG as follows. At the k-th iteration of pessimistic offline soft-DPG, with estimated pessimistic Q-function Q_k and policy π_k, we define the offline soft-DPG objective for the regularized MDP $\mathcal{M}_{\lambda_k}$ as follows,

$$\mathcal{L}_{\mathrm{DPG}}^k(\pi) = \mathbb{E}_{s \sim \mathcal{D}}\big[\langle Q_k(s, \cdot), \pi(\cdot \,|\, s)\rangle - \lambda_k \cdot \mathrm{KL}(\pi(\cdot \,|\, s) \| \pi_0(\cdot \,|\, s))\big], \tag{9}$$

where $\mathcal{D}$ is the static dataset and the KL divergence is a behavior cloning term. In policy improvement, we employ deterministic policy gradient [Silver et al., 2014] to maximize equation 9. We remark that the objective function in equation 9 is equivalent to equation 7 under Gaussian policies. While in policy evaluation, we assume that there exists an oracle that uses the ξ-uncertainty quantifier $U(s, a)$ defined in Definition 2.1 to construct a pessimistic estimator of the Q-function. Such an oracle for pessimistic evaluation can be practically achieved by equation 6 as shown in Section 3.2. Thus, our pessimistic offline soft-DPG is indeed equivalent to its practical counterpart in Algorithm 1.

Equivalence between Soft-DPG and PPO. We show that the update to maximize equation 9 is equivalent to solving the pessimistic proximal policy optimization (PPO, Schulman et al. [2015, 2017]) objective. Formally, we consider the linear function parameterization in the k-th iteration as follows,

$$\pi_{\phi_k} \propto \exp(f_{\phi_k}(s, a)), \quad f_{\phi_k}(s, a) = \psi(s, a)^\top \phi_k, \quad Q_k(s, a) = \theta_k(s, a)^\top a, \tag{10}$$

where ψ and θ_k are feature vectors, and f_{ϕ_k} is the energy function. We denote by $\pi_k = \pi_{\phi_k}$ and $f_k = f_{\phi_k}$ for notational convenience. With pessimistic Q-function Q_k and current policy π_k in the k-th iteration, we define the offline PPO objective for the regularized MDP $\mathcal{M}_{\lambda_k}$ as follows,

$$\mathcal{L}_{\mathrm{PPO}}^k(\phi) = \mathbb{E}_{s \sim \mathcal{D}}\Big[\Big\langle Q_k(s, \cdot) - \lambda_k \cdot \log \frac{\pi_\phi(\cdot \,|\, s)}{\pi_0(\cdot \,|\, s)}, \pi_\phi(\cdot \,|\, s)\Big\rangle - \eta_k \cdot \mathrm{KL}\big(\pi_\phi(\cdot \,|\, s) \| \pi_k(\cdot \,|\, s)\big)\Big], \tag{11}$$

where π_0 is the behavior policy and η_k is the regularization parameter. Under the parameterization in equation 10, we show in the following lemma that maximizing equation 11 is equivalent to a gradient update of equation 9. To introduce the lemma, we define $I_\phi = \mathbb{E}_{s \sim \mathcal{D}}[I_\phi(s)]$, where $I_\phi(s) = \mathrm{Var}_{a \sim \pi_\phi(\cdot \,|\, s)}[\psi(s, a)]$.

Lemma 3.1 (Equivalence between Soft-DPG and PPO)**.** The stationary point ϕ_{k+1} of $\mathcal{L}_{\mathrm{PPO}}^k(\phi)$ satisfies

$$\phi_{k+1} = \frac{\eta_k \phi_k + \lambda_k \phi_0}{\eta_k + \lambda_k} + (\eta_k + \lambda_k)^{-1} \cdot I_{\phi_{k+1}}^{-1} \mathbb{E}_{s \sim \mathcal{D}}\big[\nabla_a Q_k(s, \Pi_{\phi_{k+1}}(s)) \nabla_\phi \Pi_{\phi_{k+1}}(s)\big],$$

where $\Pi_\phi(s) = \mathbb{E}_{a \sim \pi_\phi(\cdot \,|\, s)}[a]$ is the deterministic policy associated with π_ϕ.

Proof. See Section B.1 for a detailed proof. □

By Lemma B.1, we see that maximizing the offline PPO objective is equivalent to an implicit natural gradient step corresponding to the maximization of the pessimistic offline soft-DPG objective. Thus, to analyze the convergence of pessimistic offline soft-DPG, it suffices to analyze pessimistic offline PPO.

Convergence Analysis. For simplicity of presentation, we take the regularization parameter $\lambda_k = \alpha^k$, where $0 < \alpha < 1$ quantifies the speed of annealing. Recall that we employ pessimism to construct estimated Q-functions Q_k at each iteration k, which ensures that there exists a ξ-uncertainty quantifier $U(s, a)$ defined in Definition 2.1. Formally, we impose the following assumption on the estimated Q-functions, which can be achieved by a bootstrapped ensemble method as shown in Section 3.2.

Assumption 3.2 (Pessimistic Q-Functions)**.** For any $k \in [K]$, $U \colon \mathcal{S} \times \mathcal{A} \to \mathbb{R}$ is a ξ-uncertainty quantifier for the estimated Q-function Q_k, i.e., the event

$$\mathcal{E}_K = \Big\{|\widehat{\mathcal{B}}Q_k(s, a) - \mathcal{B}Q_k(s, a)| \le U(s, a) \text{ for all } (s, a, k) \in \mathcal{S} \times \mathcal{A} \times [K]\Big\}$$

holds with probability at least $1 - \xi$.

We further define the pessimistic error as follows,

$$\varepsilon_{\mathrm{Pess}} = \sum_{t=0}^{\infty} 2\gamma^t \cdot \mathbb{E}_{\pi^*}\big[U(s_t, a_t) \,|\, s_0\big]. \tag{12}$$

Such a pessimistic error in equation 12 quantifies the irremovable intrinsic uncertainty. Now, we introduce our main theoretical result as follows.

Table 1: Average normalized scores over 5 random seeds on the D4RL-MuJoCo datasets. We compare SCORE with both model-based methods (MOPO, MOReL) and model-free methods (BCQ, BEAR, UWAC, CQL, TD3-BC). The standard deviation is reported in the parentheses. A score of zero corresponds to the performance of the random policy and a score of 100 corresponds to the performance of the expert policy.

Task	SCORE	MOPO	MOReL	BCQ	BEAR	UWAC	CQL	TD3-BC
halfcheetah-random	29.1±2.6	35.9±2.9	30.3±5.9	2.2±0.0	2.3±0.0	2.3±0.0	21.7±0.6	10.6±1.7
hopper-random	31.3±0.3	16.7±12.2	44.8±4.8	8.1±0.5	3.9±2.3	2.7±0.3	8.1±1.4	8.6±0.4
walker2d-random	3.7±7.0	4.2±5.7	17.3±8.2	4.6±0.7	12.8±10.2	2.0±0.4	0.5±1.3	1.5±1.4
halfcheetah-medium-replay	48.0±0.7	69.2±1.1	31.9±6.0	40.9±1.1	36.3±3.1	35.9±3.7	47.2±0.4	44.8±0.5
hopper-medium-replay	79.9±24.6	32.7±9.4	54.2±32.0	40.9±16.7	52.2±19.3	25.7±1.9	95.6±2.4	57.8±17.3
walker2d-medium-replay	84.8±1.1	73.7±2.4	13.7±8.0	42.5±13.7	7.0±7.8	23.6±6.9	85.3±2.7	81.9±2.7
halfcheetah-medium	55.2±0.4	73.1±2.4	20.4±13.8	45.4±1.7	43.0±0.2	42.1±0.5	49.2±0.3	47.8±0.4
hopper-medium	99.6±2.8	38.3±34.9	53.2±32.1	54.0±3.7	51.8±4.0	50.9±4.4	62.7±3.7	69.1±4.5
walker2d-medium	89.2±1.2	41.2±30.8	10.3±8.9	74.5±3.7	-0.2±0.1	75.4±3.0	83.3±0.8	81.3±3.0
halfcheetah-medium-expert	92.6±3.5	70.3±21.9	35.9±19.2	94.0±1.2	46.0±4.7	42.7±0.3	70.6±13.6	88.9±5.3
hopper-medium-expert	100.3±6.9	60.6±32.5	52.1±27.7	108.6±6.0	50.6±25.3	44.9±8.1	111.0±1.2	102.0±10.1
walker2d-medium-expert	109.3±0.5	77.4±27.9	3.9±2.8	109.7±0.6	22.1±44.5	96.5±9.1	109.7±0.3	110.5±0.3
halfcheetah-expert	96.4±0.6	81.3±21.8	2.2±5.4	92.7±2.5	92.7±0.6	92.9±0.6	97.5±1.8	96.3±0.9
hopper-expert	112.0±0.3	62.5±29.0	26.2±14.0	105.3±8.1	54.6±21.0	110.5±0.5	105.4±5.9	109.5±4.1
walker2d-expert	109.4±0.6	62.4±3.2	-0.3±0.3	109.0±0.4	106.8±6.8	108.4±0.4	109.0±0.4	110.3±0.4
Overall	**76.1±3.5**	53.3±16.3	26.4±12.6	62.6±4.0	38.8±10.0	50.43±2.7	70.5±2.5	68.1±3.5

Theorem 3.3. We suppose that $\lambda_k = \alpha^k$ and $\eta_k + \lambda_k = \sqrt{\zeta/K}$ for any $k \geq 0$, where

$$\zeta = \big(1 + \alpha^4(1-\alpha)^{-4}\big)^2 \cdot \sum_{t=0}^{\infty} \gamma^t \cdot \mathbb{E}_{\pi^*}\big[\mathrm{KL}\big(\pi^*(\cdot \,|\, s_t) \| \pi_0(\cdot \,|\, s_t)\big) \,|\, s_0\big],$$

Then for offline PPO with estimated Q-functions satisfying Assumption 3.2, it holds with probability at least $1 - \xi$ that

$$\mathrm{SubOptGap}(K) = O\big((1-\gamma)^{-3}\sqrt{\zeta/K}\big) + \varepsilon_{\mathrm{Pess}},$$

where $\varepsilon_{\mathrm{Pess}}$ is defined in equation 12.

Proof. See §A for a detailed proof. □

Theorem 3.3 states that the sequence of policies generated by pessimistic offline PPO converges sublinearly to an optimal policy in the regularized MDP with an additional pessimistic error term $\varepsilon_{\mathrm{Pess}}$. We remark that such an error term $\varepsilon_{\mathrm{Pess}}$ is irremovable, as it arises from the information-theoretic lower bound [Jin et al., 2021]. Moreover, given the equivalence between offline PPO and offline soft-DPG as in Lemma 3.1, we know that offline soft-DPG also converges to an optimal policy under a sublinear rate.

4 Experiments

In this section, we conduct extensive experiments on the widely adopted benchmark D4RL to verify the effectiveness of the propose algorithm. We first present the results of comparison experiments in Section 4.1. Then we visualize and analyze the uncertainty learned by our method in Section 4.2. Lastly, we perform ablation studies in Section 4.3.

4.1 Comparison Experiments

We first compare SCORE and other baselines on the D4RL-MuJoCo datasets. The experimental results in Table 1 show that SCORE obtains promising results for nearly all dataset settings. For random datasets of the lowest quality, SCORE is the only model-free algorithm that matches the performance of model-based algorithms. We can see that SCORE also works well on the medium-quality datasets. Learning from data generated by a medium-level policy, performance of SCORE is comparable to the expert policy. These results demonstrate the superiority of the pessimism principle in offline RL. For high-quality datasets, e.g., the medium-expert and expert datasets, SCORE outperforms

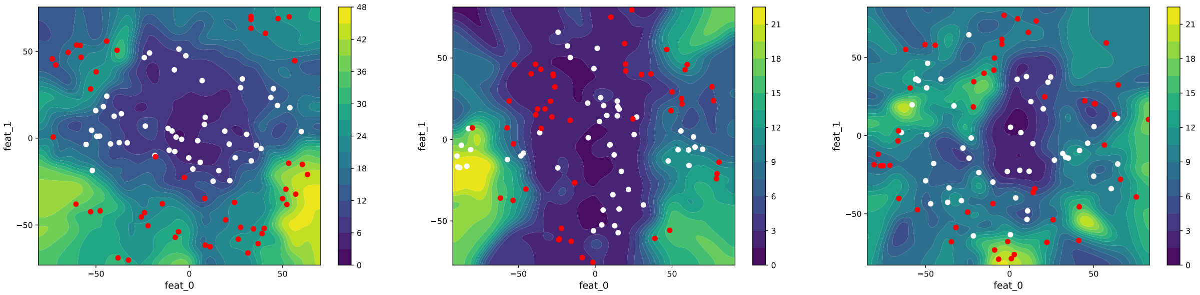

(a) halfcheetah (b) hopper (c) walker2d

Figure 2: Uncertainty estimation of the in-distribution samples (white) and OOD samples (red).

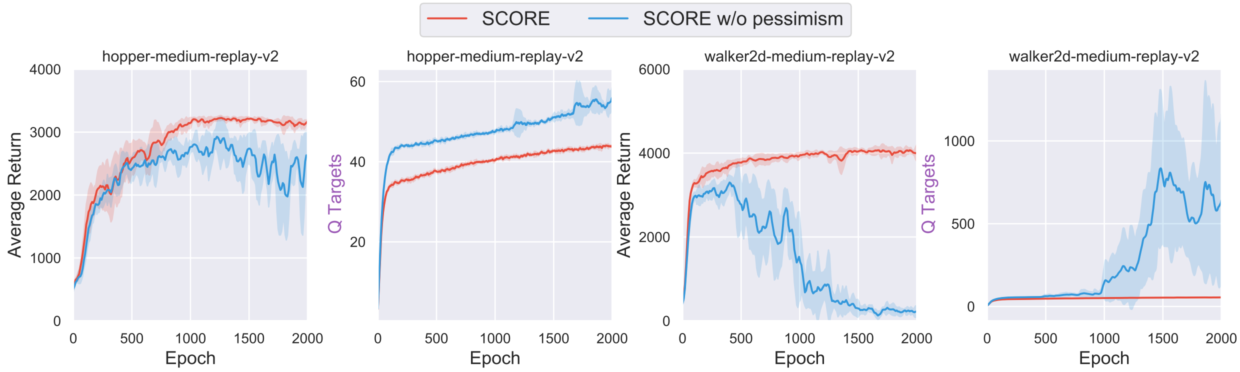

Figure 3: The average return and the Q target of SCORE vs. SCORE w/o pessimism.

model-based methods and is on par with the state-of-the-art model-free methods. Besides, we find that SCORE's performance is in line with the theory, i.e., *it improves along with the quality of the dataset* (how well the dataset covers the trajectory induced by the optimal policy). The overall performance has a considerable improvement compared to the state-of-the-art algorithms (CQL [Kumar et al., 2020] and TD3-BC [Fujimoto and Gu, 2021]).

We also conduct experiments on a more challenge task suite, D4RL-Adroit, where the datasets for these tasks have very narrow distributions and the data quality is highly unstable. Though such issues pose significant difficulties for stable uncertainty estimation, SCORE still still performs well compared with other methods. We refer to Appendix E.1 for more details of the experiments and Appendix F.1 for the experimental results on D4RL-Adroit datasets.

4.2 Visualization and Analysis of Uncertainty

To gain further insight into the uncertainty estimated by SCORE, we visualize the uncertainty. Specifically, we apply the Q functions trained on the medium-replay dataset to quantify uncertainty for different samples. We draw the in-distribution samples from the medium-replay dataset, and the OOD samples come from the expert dataset. For visualization purposes, we reduce the features of these samples to two dimensions using t-distributed stochastic neighbor embedding (t-SNE). Figure 2 shows the contour plot of the uncertainty on the two-dimensional feature space, in which the white dots denote in-distribution samples and the red dots correspond to OOD samples.

Although there are some overlaps between the two types of samples, the in-distribution samples (white) are more concentrated in regions with low uncertainty (the dark regions). On the other hand, the OOD samples (red) loosely distribute in regions with higher uncertainty (the bright regions). We can also see that the in-distribution and OOD samples are more easily distinguishable on halfcheetah, while the opposite holds for hopper and walker2d. We point out that this correlates with the performance observed in the comparison experiments (see Table 1). On halfcheetah, the performance on the medium-replay dataset is substantially lower than on the expert dataset, while it is much closer on hopper and walker2d. We suggest that this phenomenon reflects the property of the dataset, where the medium-replay datasets of hopper and walker2d have better coverage of the state-action pairs induced by the expert policy. Thus, algorithms are more likely to learn high-level policies from these medium-quality datasets.

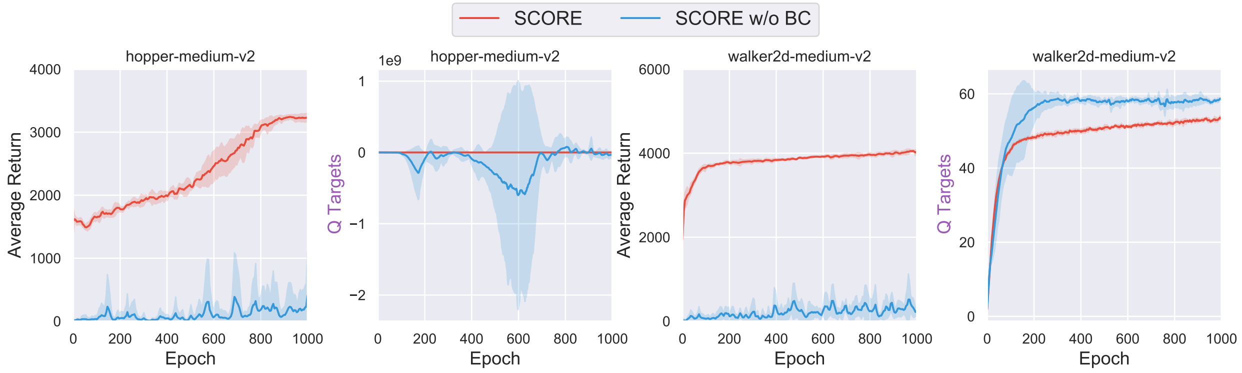

Figure 4: The average return and the Q target of SCORE vs. SCORE w/o BC on the medium datasets.

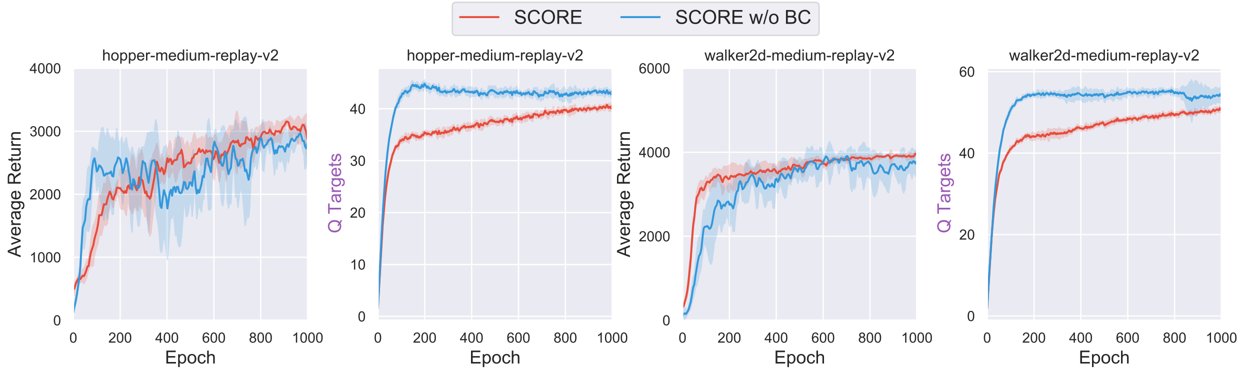

Figure 5: The average return and the Q target of SCORE vs. SCORE w/o BC on the medium-replay datasets.

4.3 Ablation Studies

Pessimism. Pessimism is the core component of the proposed method. Figure 3 shows the difference between SCORE and SCORE without pessimism (all other hyper-parameters are remained unchanged except for removing the uncertainty penalty) in a longer training period. We observe that removing pessimism may cause training instability or even severe degradation. This phenomenon is related to the Q-value, and the agent's performance is greatly affected when the Q-value jitters or explodes. The experimental results indicate that even with a good initialization (via behavior cloning), spurious correlations in offline RL can still be problematic. In contrast, pessimism is able to reduce spurious correlations and guarantees the strong empirical performance of SCORE.

Behavior Cloning. As pointed out in previous studies [Fujimoto et al., 2019, Levine et al., 2020], uncertainty-based methods cannot effectively avoid action distributional shifts. Meanwhile, estimating calibrated uncertainty for neural networks is a challenging task. Figure 4 and Figure 5 show the difference between SCORE and SCORE without BC. On datasets collected by a single policy (e.g., the medium datasets), the importance of BC goes without saying. These datasets poorly cover the state-action space, so action distributional shift is more likely to appear. By removing the regularizer, the agent fails to stay in well-supported regions. What's worse, this further affects the uncertainty estimation and makes it difficult for the agent to learn effectively. On the other hand, on datasets collected by different levels of policies (e.g., the medium-replay datasets), SCORE and SCORE without BC have similar final performance. In this case, behavior cloning serves to provide a good initialization and stabilizes the training process.

5 Related Work

Most existing works in offline RL focus on defending OOD actions, but as shown in Section 3.1, in-distribution samples can also cause detrimental effects. The *spurious correlation* arising from insufficient information of the underlying model is the main reason. To deal with this problem, most theoretical works impose various assumptions on the sufficient coverage of the dataset, e.g., the ratio between the visitation measure of the target policy and that of the behavior policy to be upper bounded uniformly over the state-action space [Xie et al., 2019, Nachum et al., 2019, Jiang and Huang, 2020, Duan et al., 2020, Zhang et al., 2020, Yin et al., 2021], or the concentrability coefficient to be upper bounded [Scherrer et al., 2015, Chen and Jiang, 2019, Liao et al., 2020, Xie and Jiang, 2021]. Until recently, without assuming sufficient coverage of the dataset, Jin et al. [2021] establishes a data-dependent upper bound on the suboptimality using pessimism. Our work adds to recent works by extending Jin et al. [2021] to regularized MDPs.

The majority of offline RL algorithms fall into two categories, i.e., policy-constrained methods and value-penalized methods. Policy-constrained methods avoid OOD actions by restricting the hypothesis space of the policy. For example, Fujimoto et al. [2019] and Ghasemipour et al. [2021] only consider actions proposed by the estimated behavioral policy. Alternatively, some methods [Wu et al., 2019, Kumar et al., 2019, Kostrikov et al., 2021, Nair et al., 2020] reformulate the policy optimization problem as a constrained optimization problem to keep the learned policy close to the behavioral policy. More recently, Fujimoto and Gu [2021] provides a simple yet effective solution by directly using the behavioral cloning loss.

On the other hand, value-penalized methods penalize the value of OOD actions to steer the policy towards well-supported regions. Kumar et al. [2020] penalizes the actions generated by the learned policy via a value regularization term. Yu et al. [2020] and Kidambi et al. [2020] learn the environmental model and then use the uncertainty in model predictions to penalize the action-values. However, in a subsequent paper [Yu et al., 2021], the authors claim that estimating uncertainty for complex models is too difficult and revert to the regularization method.

Most of the current uncertainty-based approaches belong to model-based methods. Since the model is learned in a supervised manner, it provides much stable uncertainty estimation. However, as shown in the comparison experiments in Section 4, their performance heavily rely on sufficient coverage of the state-action space, which in many cases is impractical. In contrast, SCORE utilizes bootstrapped ensembles to estimate uncertainty, avoiding model learning while still providing reliable uncertainty estimations. A recent work UWAC [Wu et al., 2021] proposes to use Monte Carlo dropout (MC dropout) to estimate uncertainty and perform weighted updates to the critics and the policy. While this method is also model-free, it relies on a strong policy-constrained method. More importantly, *the dropout method does not converge with increasing data* [Osband et al., 2018]. In contrast, our method reduces to a pure uncertainty-based method when the regularization λ decays to zero, and the uncertainty decreases to zero with more data, enjoying a solid theoretical foundation.

6 Conclusion

In this work, we emphasize that spurious correlations stem from insufficient information about the environment is a core problem in Offline RL. We propose a simple and principled algorithm named SCORE to address this problem. The effectiveness of SCORE is verified by both theoretical analyses and empirical studies.

Our work is nicely complementary to recent theoretical studies in offline RL. It suggests that pessimism is not only provably efficient but also helps to improve performance in practice. We remark spurious correlations are not always detrimental. How to avoid over-pessimism and how to further improve the policy in the real environment with a small number of online interactions are the main focuses of our future research.

References

Scott Fujimoto, David Meger, and Doina Precup. Off-policy deep reinforcement learning without exploration. In *International Conference on Machine Learning*, pages 2052–2062. PMLR, 2019.

Justin Fu, Aviral Kumar, Ofir Nachum, George Tucker, and Sergey Levine. D4RL: Datasets for deep data-driven reinforcement learning. *arXiv preprint arXiv:2004.07219*, 2020.

Yifan Wu, George Tucker, and Ofir Nachum. Behavior regularized offline reinforcement learning. *arXiv preprint arXiv:1911.11361*, 2019.

Sergey Levine, Aviral Kumar, George Tucker, and Justin Fu. Offline reinforcement learning: Tutorial, review, and perspectives on open problems. *arXiv preprint arXiv:2005.01643*, 2020.

Ying Jin, Zhuoran Yang, and Zhaoran Wang. Is pessimism provably efficient for offline rl? In *International Conference on Machine Learning*, pages 5084–5096. PMLR, 2021.

Tengyang Xie, Ching-An Cheng, Nan Jiang, Paul Mineiro, and Alekh Agarwal. Bellman-consistent pessimism for offline reinforcement learning. *arXiv preprint arXiv:2106.06926*, 2021.

Tianhe Yu, Aviral Kumar, Rafael Rafailov, Aravind Rajeswaran, Sergey Levine, and Chelsea Finn. COMBO: Conservative offline model-based policy optimization. *arXiv:2102.08363 [cs]*, February 2021.

Aviral Kumar, Justin Fu, George Tucker, and Sergey Levine. Stabilizing off-policy q-learning via bootstrapping error reduction. *arXiv preprint arXiv:1906.00949*, 2019.

Aviral Kumar, Aurick Zhou, George Tucker, and Sergey Levine. Conservative Q-learning for offline reinforcement learning. *arXiv preprint arXiv:2006.04779*, 2020.

Ian Osband, Charles Blundell, Alexander Pritzel, and Benjamin Van Roy. Deep exploration via bootstrapped DQN. In *Advances in Neural Information Processing Systems*, volume 29. Curran Associates, Inc., 2016.

Balaji Lakshminarayanan, Alexander Pritzel, and Charles Blundell. Simple and scalable predictive uncertainty estimation using Deep Ensembles. *arXiv:1612.01474 [cs, stat]*, November 2017.

Ian Osband, John Aslanides, and Albin Cassirer. Randomized prior functions for deep reinforcement learning. *arXiv:1806.03335 [cs, stat]*, November 2018.

Yue Wu, Shuangfei Zhai, Nitish Srivastava, Joshua Susskind, Jian Zhang, Ruslan Salakhutdinov, and Hanlin Goh. Uncertainty Weighted Actor-Critic for offline reinforcement learning. *arXiv preprint arXiv:2105.08140*, 2021.

Yijie Guo, Shengyu Feng, Nicolas Le Roux, Honglak Lee, and Minmin Chen. Batch reinforcement learning through continuation method. In *International Conference on Learning Representations*, 2020.

John Schulman, Sergey Levine, Pieter Abbeel, Michael Jordan, and Philipp Moritz. Trust region policy optimization. In *International conference on machine learning*, pages 1889–1897. PMLR, 2015.

John Schulman, Filip Wolski, Prafulla Dhariwal, Alec Radford, and Oleg Klimov. Proximal policy optimization algorithms. *arXiv preprint arXiv:1707.06347*, 2017.

David Silver, Guy Lever, Nicolas Heess, Thomas Degris, Daan Wierstra, and Martin Riedmiller. Deterministic policy gradient algorithms. In *International conference on machine learning*, pages 387–395. PMLR, 2014.

Scott Fujimoto and Shixiang Shane Gu. A minimalist approach to offline reinforcement learning. *arXiv preprint arXiv:2106.06860*, 2021.

Tengyang Xie, Yifei Ma, and Yu-Xiang Wang. Towards optimal off-policy evaluation for reinforcement learning with marginalized importance sampling. *arXiv preprint arXiv:1906.03393*, 2019.

Ofir Nachum, Yinlam Chow, Bo Dai, and Lihong Li. Dualdice: Behavior-agnostic estimation of discounted stationary distribution corrections. *arXiv preprint arXiv:1906.04733*, 2019.

Nan Jiang and Jiawei Huang. Minimax value interval for off-policy evaluation and policy optimization. *arXiv preprint arXiv:2002.02081*, 2020.

Yaqi Duan, Zeyu Jia, and Mengdi Wang. Minimax-optimal off-policy evaluation with linear function approximation. In *International Conference on Machine Learning*, pages 2701–2709. PMLR, 2020.

Ruiyi Zhang, Bo Dai, Lihong Li, and Dale Schuurmans. Gendice: Generalized offline estimation of stationary values. *arXiv preprint arXiv:2002.09072*, 2020.

Ming Yin, Yu Bai, and Yu-Xiang Wang. Near-optimal provable uniform convergence in offline policy evaluation for reinforcement learning. In *International Conference on Artificial Intelligence and Statistics*, pages 1567–1575. PMLR, 2021.

Bruno Scherrer, Mohammad Ghavamzadeh, Victor Gabillon, Boris Lesner, and Matthieu Geist. Approximate modified policy iteration and its application to the game of tetris. *J. Mach. Learn. Res.*, 16:1629–1676, 2015.

Jinglin Chen and Nan Jiang. Information-theoretic considerations in batch reinforcement learning. In *International Conference on Machine Learning*, pages 1042–1051. PMLR, 2019.

Peng Liao, Zhengling Qi, and Susan Murphy. Batch policy learning in average reward markov decision processes. *arXiv preprint arXiv:2007.11771*, 2020.

Tengyang Xie and Nan Jiang. Batch value-function approximation with only realizability. In *International Conference on Machine Learning*, pages 11404–11413. PMLR, 2021.

Seyed Kamyar Seyed Ghasemipour, Dale Schuurmans, and Shixiang Shane Gu. EMaQ: Expected-Max Q-learning operator for simple yet effective offline and online rl. In *International Conference on Machine Learning*, pages 3682–3691. PMLR, 2021.

Ilya Kostrikov, Rob Fergus, Jonathan Tompson, and Ofir Nachum. Offline reinforcement learning with fisher divergence critic regularization. In *International Conference on Machine Learning*, pages 5774–5783. PMLR, 2021.

Ashvin Nair, Murtaza Dalal, Abhishek Gupta, and Sergey Levine. Accelerating online reinforcement learning with offline datasets. *arXiv preprint arXiv:2006.09359*, 2020.

Tianhe Yu, Garrett Thomas, Lantao Yu, Stefano Ermon, James Zou, Sergey Levine, Chelsea Finn, and Tengyu Ma. MOPO: Model-based offline policy optimization. *arXiv preprint arXiv:2005.13239*, 2020.

Rahul Kidambi, Aravind Rajeswaran, Praneeth Netrapalli, and Thorsten Joachims. MOReL: Model-based offline reinforcement learning. *arXiv preprint arXiv:2005.05951*, 2020.

Qi Cai, Zhuoran Yang, Chi Jin, and Zhaoran Wang. Provably efficient exploration in policy optimization. In *International Conference on Machine Learning*, pages 1283–1294. PMLR, 2020.

Steven J Bradtke and Andrew G Barto. Linear least-squares algorithms for temporal difference learning. *Machine learning*, 22(1):33–57, 1996.

Francisco S Melo and M Isabel Ribeiro. Q-learning with linear function approximation. In *International Conference on Computational Learning Theory*, pages 308–322. Springer, 2007.

Scott Fujimoto, Herke Hoof, and David Meger. Addressing function approximation error in actor-critic methods. In *International Conference on Machine Learning*, pages 1587–1596. PMLR, 2018.

A Proof of Theorem 3.3

Proof. We denote by

$$\text{AveSubOptGap}(K) = \frac{1}{K} \cdot \sum_{k=0}^{K-1} \big(V_k^*(s_0) - V_k^{\pi_k}(s_0)\big). \tag{13}$$

By the definition of $\text{SubOptGap}(K)$ in equation 8, we know that $\text{SubOptGap}(K) \le \text{AveSubOptGap}(K)$. Before we prove the theorem, we first introduce the following useful lemmas.

Lemma A.1 (Suboptimality Decomposition)**.** For $\text{AveSubOptGap}(K)$ defined in equation 13, we have

$$\begin{aligned}\text{AveSubOptGap}(K) = \frac{1}{K} \cdot \sum_{k=0}^{K-1} \sum_{t=0}^{\infty} \gamma^t \cdot \Big(&\mathbb{E}_{\pi^*}\Big[\Big\langle Q_k(s_t, \cdot) - \lambda_k \cdot \log \frac{\pi_k(\cdot \,|\, s_t)}{\pi_0(\cdot \,|\, s_t)}, \pi^*(\cdot \,|\, s_t) - \pi_k(\cdot \,|\, s_t)\Big\rangle \,\Big|\, s_0\Big] \\ &+ \mathbb{E}_{\pi^*}\big[\iota_k(s_t, a_t) \,|\, s_0\big] - \mathbb{E}_{\pi_k}\big[\iota_k(s_t, a_t) \,|\, s_0\big]\Big),\end{aligned}$$

where $\iota_k(s, a) = r(s, a) + \gamma \cdot \mathbb{E}_{s' \sim \mathcal{P}(\cdot \,|\, s,a)}[V_k(s')] - Q_k(s, a)$ for any $(s, a) \in \mathcal{S} \times \mathcal{A}$.

Proof. See proof of Lemma 4.2 in Cai et al. [2020] for a detailed proof. □

Lemma A.2 (Policy Improvement)**.** It holds for any k that

$$\begin{aligned}&(\eta_k + \lambda_k)^{-1} \cdot \Big\langle Q_k(s_t, \cdot) - \lambda_k \cdot \log \frac{\pi_k(\cdot \,|\, s_t)}{\pi_0(\cdot \,|\, s_t)}, \pi^*(\cdot \,|\, s_t) - \pi_k(\cdot \,|\, s_t)\Big\rangle \\ &\quad \le \text{KL}\big(\pi^*(\cdot \,|\, s_t) \| \pi_k(\cdot \,|\, s_t)\big) - \text{KL}\big(\pi^*(\cdot \,|\, s_t) \| \pi_{k+1}(\cdot \,|\, s_t)\big) \\ &\qquad + (\eta_k + \lambda_k)^{-2} \cdot \big(1 + \lambda_k \cdot \alpha^4 (1 - \alpha)^{-4}\big)^2 \cdot (1 - \gamma)^{-2}.\end{aligned}$$

Proof. See Section B.2 for a detailed proof. □

Lemma A.3 (Pessimism)**.** Under Assumption 3.2, with probability at least $1-\xi$, it holds for any $(s, a, k) \in \mathcal{S} \times \mathcal{A} \times [K]$ that

$$0 \le \iota_k(s, a) \le 2U(s, a),$$

where $\iota_k = \mathcal{B}Q_k - \widehat{\mathcal{B}}Q_k$ is the epistemic error defined in equation 1.

Proof. See proof of Lemma 5.1 in Jin et al. [2021] for a detailed proof. □

Now we prove the theorem. By Lemma A.1, we have

$$\begin{aligned}\text{AveSubOptGap}(K) &= \frac{1}{K} \cdot \sum_{k=0}^{K} \sum_{t=0}^{\infty} \gamma^t \cdot \Big(\mathbb{E}_{\pi^*}\Big[\Big\langle Q_k(s_t, \cdot) - \lambda_k \cdot \log \frac{\pi_k(\cdot \,|\, s_t)}{\pi_0(\cdot \,|\, s_t)}, \pi^*(\cdot \,|\, s_t) - \pi_k(\cdot \,|\, s_t)\Big\rangle \,\Big|\, s_0\Big] \\ &\qquad + \mathbb{E}_{\pi^*}\big[\iota_k(s_t, a_t) \,|\, s_0\big] - \mathbb{E}_{\pi_k}\big[\iota_k(s_t, a_t) \,|\, s_0\big]\Big) \\ &\le \frac{1}{K} \cdot \sum_{k=0}^{K} \sum_{t=0}^{\infty} \gamma^t \cdot \Big(\mathbb{E}_{\pi^*}\big[\eta \cdot \text{KL}\big(\pi^*(\cdot \,|\, s_t) \| \pi_k(\cdot \,|\, s_t)\big) - \eta \cdot \text{KL}\big(\pi^*(\cdot \,|\, s_t) \| \pi_{k+1}(\cdot \,|\, s_t)\big)\big] \\ &\qquad + \eta^{-1} \cdot \big(1 + \lambda_k \cdot \alpha^4 (1 - \alpha)^{-4}\big)^2 \cdot (1 - \gamma)^{-2} \\ &\qquad + \mathbb{E}_{\pi^*}\big[\iota_k(s_t, a_t) \,|\, s_0\big] - \mathbb{E}_{\pi_k}\big[\iota_k(s_t, a_t) \,|\, s_0\big]\Big),\end{aligned} \tag{14}$$

where the last inequality comes from Lemma A.2. Further, by telescoping the sum of k on the right-hand side of equation 14 and the non-negativity of the KL divergence, it holds with probability at least $1-\xi$ that

$$\begin{aligned}\text{AveSubOptGap}(K) &\leq \frac{\eta}{K}\cdot\sum_{t=0}^{\infty}\gamma^t\cdot\mathbb{E}_{\pi^*}\big[\text{KL}\big(\pi^*(\cdot\,|\,s_t)\|\pi_0(\cdot\,|\,s_t)\big)\big]+\eta^{-1}\cdot\big(1+\alpha^4(1-\alpha)^{-4}\big)^2\cdot(1-\gamma)^{-3}\\ &\quad+\frac{1}{K}\cdot\sum_{k=0}^{K}\sum_{t=0}^{\infty}\gamma^t\cdot\Big(\mathbb{E}_{\pi^*}\big[\iota_k(s_t,a_t)\,|\,s_0\big]-\mathbb{E}_{\pi_k}\big[\iota_k(s_t,a_t)\,|\,s_0\big]\Big)\\ &\leq \frac{\eta}{K}\cdot\sum_{t=0}^{\infty}\gamma^t\cdot\mathbb{E}_{\pi^*}\big[\text{KL}\big(\pi^*(\cdot\,|\,s_t)\|\pi_0(\cdot\,|\,s_t)\big)\big]+\eta^{-1}\cdot\big(1+\alpha^4(1-\alpha)^{-4}\big)^2\cdot(1-\gamma)^{-3}\\ &\quad+\sum_{t=0}^{\infty}\gamma^t\cdot\mathbb{E}_{\pi^*}\big[2U(s_t,a_t)\,|\,s_0\big],\end{aligned}\tag{15}$$

where the last inequality comes from Lemma A.3. Now, by taking $\eta=\sqrt{\zeta/K}$, where

$$\zeta=\big(1+\alpha^4(1-\alpha)^{-4}\big)^2\cdot\sum_{t=0}^{\infty}\gamma^t\cdot\mathbb{E}_{\pi^*}\big[\text{KL}\big(\pi^*(\cdot\,|\,s_t)\|\pi_0(\cdot\,|\,s_t)\big)\big],$$

combining equation 15, with probability at least $1-\xi$, we have

$$\text{AveSubOptGap}(K)=O\big((1-\gamma)^{-3}\sqrt{\zeta/K}\big)+\varepsilon_{\text{Pess}}.$$

Here $\varepsilon_{\text{Pess}}$ is the intrinsic uncertainty defined in equation 12. By the fact that $\text{SubOptGap}(K)\leq\text{AveSubOptGap}(K)$, we conclude the proof. □

B Proof of Lemmas

B.1 Proof of Lemma 3.1

Proof. By plugging the definition of $\Pi_\phi(s) = \mathbb{E}_{a\sim\pi_\phi(\cdot\,|\,s)}[a]$ and the linear parameterization $Q_k(s,a) = \theta_k(s,a)^\top a$ into equation 11, we have

$$\mathcal{L}^k_{\mathrm{PPO}}(\phi) = \mathbb{E}_{s\sim\mathcal{D}}\big[Q_k(s,\Pi_\phi(s)) - \lambda_k\cdot \mathrm{KL}(\pi_\phi(\cdot\,|\,s)\|\pi_0(\cdot\,|\,s)) - \eta_k\cdot\mathrm{KL}(\pi_\phi(\cdot\,|\,s)\|\pi_k(\cdot\,|\,s))\big]. \tag{16}$$

It holds for any $s\in\mathcal{S}$ that

$$\begin{aligned}\nabla_\phi \mathrm{KL}(\pi_\phi(\cdot\,|\,s)\|\pi_0(\cdot\,|\,s)) &= \nabla_\phi\mathbb{E}_{a\sim\pi_\phi(\cdot\,|\,s)}\Big[\log\big(\pi_\phi(a\,|\,s)/\pi_0(a\,|\,s)\big)\Big]\\ &= \nabla_\phi\mathbb{E}_{a\sim\pi_\phi(\cdot\,|\,s)}\big[(\phi-\phi_0)^\top\psi(s,a) + Z_\phi(s) - Z_{\phi_0}(s)\big]\\ &= \nabla_\phi\mathbb{E}_{a\sim\pi_\phi(\cdot\,|\,s)}[\psi(s,a)](\phi-\phi_0) + \mathbb{E}_{a\sim\pi_\phi(\cdot\,|\,s)}[\psi(s,a)] - \nabla_\phi Z_\phi(s)\\ &= \nabla^2_\phi Z_\phi(s)(\phi-\phi_0) = \mathrm{Var}_{a\sim\pi_\phi(\cdot\,|\,s)}[\psi(s,a)](\phi-\phi_0)\\ &= I_\phi(s)(\phi-\phi_0).\end{aligned} \tag{17}$$

Similarly, we have

$$\nabla_\phi\mathrm{KL}(\pi_\phi(\cdot\,|\,s)\|\pi_k(\cdot\,|\,s)) = I_\phi(s)(\phi-\phi_k). \tag{18}$$

for any $s\in\mathcal{S}$. Thus, by combining equation 16, equation 17, and equation 18, the stationary point ϕ_{k+1} of $\mathcal{L}^k_{\mathrm{PPO}}(\phi)$ satisfies

$$\begin{aligned}\mathbb{E}_{s\sim\mathcal{D}}\Big[\nabla_a Q_k(s,\Pi_{\phi_{k+1}}(s))\nabla_\phi\Pi_{\phi_{k+1}}(s) - \lambda_k\cdot I_{\phi_{k+1}}(s)(\phi_{k+1}-\phi_0)&\\ -\eta_k\cdot I_{\phi_{k+1}}(s)(\phi_{k+1}-\phi_k)\Big] &= 0.\end{aligned} \tag{19}$$

Now, by equation 19, we have

$$\phi_{k+1} = \frac{\eta_k\phi_k + \lambda_k\phi_0}{\eta_k+\lambda_k} + (\eta_k+\lambda_k)^{-1}\cdot I^{-1}_{\phi_{k+1}}\mathbb{E}_{s\sim\mathcal{D}}\big[\nabla_a Q_k(s,\Pi_{\phi_{k+1}}(s))\nabla_\phi\Pi_{\phi_{k+1}}(s)\big],$$

which concludes the proof. □

B.2 Proof of Lemma A.2

Proof. First, by maximizing equation 11, we have

$$\pi_{k+1}(a\,|\,s) \propto \exp\{(\eta_k+\lambda_k)^{-1}\cdot(Q_k(s,a) + \eta_k f_k(s,a) + \lambda_k f_0(s,a))\}.$$

Thus, for any policy π' and π'', it holds for any $s\in\mathcal{S}$ that

$$\begin{aligned}&\Big\langle \log\frac{\pi_{k+1}(\cdot\,|\,s)}{\pi_k(\cdot\,|\,s)}, \pi'(\cdot\,|\,s) - \pi''(\cdot\,|\,s)\Big\rangle\\ &\qquad = (\eta_k+\lambda_k)^{-1}\cdot\Big\langle Q_k(s,\cdot) - \lambda_k\cdot\log\frac{\pi_k(\cdot\,|\,s)}{\pi_0(\cdot\,|\,s)}, \pi'(\cdot\,|\,s)-\pi''(\cdot\,|\,s)\Big\rangle.\end{aligned} \tag{20}$$

We will use equation 20 in the following proof.

Note that

$$\begin{aligned}&\mathrm{KL}\big(\pi^*(\cdot\,|\,s_t)\|\pi_k(\cdot\,|\,s_t)\big) - \mathrm{KL}\big(\pi^*(\cdot\,|\,s_t)\|\pi_{k+1}(\cdot\,|\,s_t)\big)\\ &\quad = \Big\langle\log\frac{\pi_{k+1}(\cdot\,|\,s_t)}{\pi_k(\cdot\,|\,s_t)}, \pi^*(\cdot\,|\,s_t)\Big\rangle\\ &\quad = \Big\langle\log\frac{\pi_{k+1}(\cdot\,|\,s_t)}{\pi_k(\cdot\,|\,s_t)}, \pi^*(\cdot\,|\,s_t) - \pi_{k+1}(\cdot\,|\,s_t)\Big\rangle + \mathrm{KL}\big(\pi_{k+1}(\cdot\,|\,s_t)\|\pi_k(\cdot\,|\,s_t)\big).\end{aligned} \tag{21}$$

In the meanwhile, we have

$$
\begin{aligned}
&\Big\langle \log \frac{\pi_{k+1}(\cdot \,|\, s_t)}{\pi_k(\cdot \,|\, s_t)}, \pi^*(\cdot \,|\, s_t) - \pi_{k+1}(\cdot \,|\, s_t) \Big\rangle \\
&\quad = \Big\langle \log \frac{\pi_{k+1}(\cdot \,|\, s_t)}{\pi_k(\cdot \,|\, s_t)}, \pi^*(\cdot \,|\, s_t) - \pi_k(\cdot \,|\, s_t) \Big\rangle + \Big\langle \log \frac{\pi_{k+1}(\cdot \,|\, s_t)}{\pi_k(\cdot \,|\, s_t)}, \pi_k(\cdot \,|\, s_t) - \pi_{k+1}(\cdot \,|\, s_t) \Big\rangle \\
&\quad = (\eta_k + \lambda_k)^{-1} \cdot \Big\langle Q_k(s_t, \cdot) - \lambda_k \cdot \log \frac{\pi_k(\cdot \,|\, s_t)}{\pi_0(\cdot \,|\, s_t)}, \pi^*(\cdot \,|\, s_t) - \pi_k(\cdot \,|\, s_t) \Big\rangle \\
&\qquad + (\eta_k + \lambda_k)^{-1} \cdot \Big\langle Q_k(s_t, \cdot) - \lambda_k \cdot \log \frac{\pi_k(\cdot \,|\, s_t)}{\pi_0(\cdot \,|\, s_t)}, \pi_k(\cdot \,|\, s_t) - \pi_{k+1}(\cdot \,|\, s_t) \Big\rangle, \qquad (22)
\end{aligned}
$$

where the last equality comes from equation 20. Combining equation 21 and equation 22, we have

$$
\begin{aligned}
&(\eta_k + \lambda_k)^{-1} \cdot \Big\langle Q_k(s_t, \cdot) - \lambda_k \cdot \log \frac{\pi_k(\cdot \,|\, s_t)}{\pi_0(\cdot \,|\, s_t)}, \pi^*(\cdot \,|\, s_t) - \pi_k(\cdot \,|\, s_t) \Big\rangle \\
&\quad = \mathrm{KL}\big(\pi^*(\cdot \,|\, s_t) \| \pi_k(\cdot \,|\, s_t)\big) - \mathrm{KL}\big(\pi^*(\cdot \,|\, s_t) \| \pi_{k+1}(\cdot \,|\, s_t)\big) - \mathrm{KL}\big(\pi_{k+1}(\cdot \,|\, s_t) \| \pi_k(\cdot \,|\, s_t)\big) \\
&\qquad - (\eta_k + \lambda_k)^{-1} \cdot \Big\langle Q_k(s_t, \cdot) - \lambda_k \cdot \log \frac{\pi_k(\cdot \,|\, s_t)}{\pi_0(\cdot \,|\, s_t)}, \pi_k(\cdot \,|\, s_t) - \pi_{k+1}(\cdot \,|\, s_t) \Big\rangle \\
&\quad \le \mathrm{KL}\big(\pi^*(\cdot \,|\, s_t) \| \pi_k(\cdot \,|\, s_t)\big) - \mathrm{KL}\big(\pi^*(\cdot \,|\, s_t) \| \pi_{k+1}(\cdot \,|\, s_t)\big) - \big\| \pi_{k+1}(\cdot \,|\, s_t) - \pi_k(\cdot \,|\, s_t) \big\|_1^2 / 2 \\
&\qquad - (\eta_k + \lambda_k)^{-1} \cdot \Big\langle Q_k(s_t, \cdot) - \lambda_k \cdot \log \frac{\pi_k(\cdot \,|\, s_t)}{\pi_0(\cdot \,|\, s_t)}, \pi_k(\cdot \,|\, s_t) - \pi_{k+1}(\cdot \,|\, s_t) \Big\rangle, \qquad (23)
\end{aligned}
$$

where the last inequality comes from Pinsker's inequality. To upper bound the last term on the right-hand side of equation 23, we characterize $\log(\pi_k(a \,|\, s)/\pi_0(a \,|\, s))$ as follows.

Characterization of $\log(\pi_k/\pi_0)$**.** For any $(s, a) \in \mathcal{S} \times \mathcal{A}$, we have

$$
\log \frac{\pi_k}{\pi_0} = \log\Big(\frac{\pi_k}{\pi_{k-1}} \cdot \frac{\pi_{k-1}}{\pi_{k-2}} \cdot \dots \cdot \frac{\pi_1}{\pi_0} \Big) = \sum_{i=0}^{k-1} \log \frac{\pi_{i+1}}{\pi_i}.
$$

Then, we have

$$
\log \frac{\pi_k}{\pi_0} = \sum_{i=0}^{k-1} \log \frac{\pi_{i+1}}{\pi_i} = \sum_{i=0}^{k-1} \Big(Q_i + \lambda_i \cdot \log \frac{\pi_i}{\pi_0} \Big) + Z_1, \qquad (24)
$$

where Z_1 is a function independent of a. Now, by recursively applying equation 24, we have

$$
\log \frac{\pi_k}{\pi_0} = \sum_{i=0}^{k-1} Q_i \cdot \sum_{j=i+1}^{k} \lambda_j \Big(1 + \sum_{\ell=0}^{k-j-1} \varepsilon_\ell \prod_{p=0}^{\ell} \lambda_{k-p} \Big) + Z_2, \qquad (25)
$$

where ε_ℓ is either 1 or -1, and Z_2 is a function independent of a.

Now, by equation 25, the last term on the right-hand side of equation 23 can be upper bounded as follows,

$$
\begin{aligned}
&- (\eta_k + \lambda_k)^{-1} \cdot \Big\langle Q_k(s_t, \cdot) - \lambda_k \cdot \log \frac{\pi_k(\cdot \,|\, s_t)}{\pi_0(\cdot \,|\, s_t)}, \pi_k(\cdot \,|\, s_t) - \pi_{k+1}(\cdot \,|\, s_t) \Big\rangle \\
&\quad = -(\eta_k + \lambda_k)^{-1} \cdot \Big\langle Q_k(s_t, \cdot) - \lambda_k \sum_{i=0}^{k-1} Q_i(s_t, \cdot) \sum_{j=i+1}^{k} \lambda_j \Big(1 + \sum_{\ell=0}^{k-j-1} \varepsilon_\ell \prod_{p=0}^{\ell} \lambda_{k-p} \Big) - \lambda_k \cdot Z_2(s_t), \\
&\qquad\qquad \pi_k(\cdot \,|\, s_t) - \pi_{k+1}(\cdot \,|\, s_t) \Big\rangle \\
&\quad = -(\eta_k + \lambda_k)^{-1} \cdot \Big\langle Q_k(s_t, \cdot) - \lambda_k \sum_{i=0}^{k-1} Q_i(s_t, \cdot) \sum_{j=i+1}^{k} \lambda_j \Big(1 + \sum_{\ell=0}^{k-j-1} \varepsilon_\ell \prod_{p=0}^{\ell} \lambda_{k-p} \Big), \\
&\qquad\qquad \pi_k(\cdot \,|\, s_t) - \pi_{k+1}(\cdot \,|\, s_t) \Big\rangle \\
&\quad \le (\eta_k + \lambda_k)^{-1} \cdot \Big\| Q_k(s_t, \cdot) - \lambda_k \sum_{i=0}^{k-1} Q_i(s_t, \cdot) \sum_{j=i+1}^{k} \lambda_j \Big(1 + \sum_{\ell=0}^{k-j-1} \varepsilon_\ell \prod_{p=0}^{\ell} \lambda_{k-p} \Big) \Big\|_\infty \qquad (26) \\
&\qquad\qquad \cdot \| \pi_k(\cdot \,|\, s_t) - \pi_{k+1}(\cdot \,|\, s_t) \|_1,
\end{aligned}
$$

where the last line comes from Hölder's inequality. In the meanwhile, it holds that

$$\|Q_k\|_\infty \le (1-\gamma)^{-1}, \tag{27}$$

and

$$\Big\|\sum_{i=0}^{k-1} Q_i(s_t,\cdot) \sum_{j=i+1}^{k} \lambda_j \Big(1 + \sum_{\ell=0}^{k-j-1} \varepsilon_\ell \prod_{p=0}^{\ell} \lambda_{k-p}\Big)\Big\|_\infty \le \alpha^4(1-\alpha)^{-4}(1-\gamma)^{-1}. \tag{28}$$

Now, by plugging equation 27 and equation 28 into equation 26, we have

$$\begin{aligned}
&(\eta_k+\lambda_k)^{-1} \cdot \Big\langle Q_k(s_t,\cdot) - \lambda_k \cdot \log \frac{\pi_k(\cdot \,|\, s_t)}{\pi_0(\cdot \,|\, s_t)}, \pi_k(\cdot \,|\, s_t) - \pi_{k+1}(\cdot \,|\, s_t)\Big\rangle \\
&\qquad \le (\eta_k+\lambda_k)^{-1} \cdot (1+\lambda_k\alpha^4(1-\alpha)^{-4})(1-\gamma)^{-1} \cdot \|\pi_k(\cdot \,|\, s_t) - \pi_{k+1}(\cdot \,|\, s_t)\|_1.
\end{aligned} \tag{29}$$

Now, combining equation 23 and equation 29, it holds that

$$\begin{aligned}
&(\eta_k+\lambda_k)^{-1} \cdot \Big\langle Q_k(s_t,\cdot) - \lambda_k \cdot \log \frac{\pi_k(\cdot \,|\, s_t)}{\pi_0(\cdot \,|\, s_t)}, \pi^*(\cdot \,|\, s_t) - \pi_k(\cdot \,|\, s_t)\Big\rangle \\
&\quad \le \mathrm{KL}\big(\pi^*(\cdot \,|\, s_t)\|\pi_k(\cdot \,|\, s_t)\big) - \mathrm{KL}\big(\pi^*(\cdot \,|\, s_t)\|\pi_{k+1}(\cdot \,|\, s_t)\big) - \big\|\pi_{k+1}(\cdot \,|\, s_t) - \pi_k(\cdot \,|\, s_t)\big\|_1^2/2 \\
&\qquad + (\eta_k+\lambda_k)^{-1} \cdot (1+\lambda_k\alpha^4(1-\alpha)^{-4})(1-\gamma)^{-1} \cdot \|\pi_k(\cdot \,|\, s_t) - \pi_{k+1}(\cdot \,|\, s_t)\|_1 \\
&\quad \le \mathrm{KL}\big(\pi^*(\cdot \,|\, s_t)\|\pi_k(\cdot \,|\, s_t)\big) - \mathrm{KL}\big(\pi^*(\cdot \,|\, s_t)\|\pi_{k+1}(\cdot \,|\, s_t)\big) \\
&\qquad + (\eta_k+\lambda_k)^{-2} \cdot \big(1+\lambda_k \cdot \alpha^4(1-\alpha)^{-4}\big)^2 \cdot (1-\gamma)^{-2},
\end{aligned}$$

which concludes the proof. □

C Theoretical Connections between SCORE and PEVI [Jin et al., 2021]

Jin et al. [2021] propose a provably efficient offline RL algorithm named PEssimistic Value Iteration (PEVI) for linear MDPs [Bradtke and Barto, 1996, Melo and Ribeiro, 2007]. PEVI eliminates spurious correlations and achieves minimax optimal. In this section, we show that the uncertainty in SCORE is theoretically equivalent to the one used by PEVI. Therefore, SCORE is also supported by the theoretical results of PEVI.

In linear MDPs, there exist a known feature map $\phi : \mathcal{S} \times \mathcal{A} \to \mathbb{R}^d$ such that the state transition function and the reward function can be parameterized in a linear manner. Suppose $Q_h(s_h, a_h) = w_h^T \phi(s_h, a_h)$, the parameter $w_h \in \mathbb{R}^d$ can be estimated by solving the following a regularized least-squares problem given the dataset $\mathcal{D}$:

$$\widehat{w}_h \to \arg\min_{w} \sum_{i=1}^{N} \left[y^{(i)} - w^T \phi(s_h^{(i)}, a_h^{(i)}) \right]^2 + \lambda \|w\|^2, \tag{30}$$

where $y^{(i)} = r_h(s_h^{(i)}, a_h^{(i)}) + \max_a Q_{h+1}(s_h^{(i)}, a)$ and λ denotes the regularization coefficient. The analytical solution of equation 30 is:

$$\begin{aligned} \widehat{w}_h &= \Lambda_h^{-1} \left(\sum_{1}^{N} \phi(s_h^{(i)}, a_h^{(i)}) \cdot \left(r_h(s_h^{(i)}, a_h^{(i)}) + \max_a Q_{h+1}(s_h^{(i)}, a) \right) \right), \\ \Lambda_h &= \sum_{1}^{N} \phi(s_h^{(i)}, a_h^{(i)}) \phi(s_h^{(i)}, a_h^{(i)})^T + \lambda \cdot \mathrm{I}. \end{aligned} \tag{31}$$

Here I denotes the identity matrix. PEVI proposes to construct the uncertainty quantifier defined in Definition 2.1 as

$$U_h(s_h^{(i)}, a_h^{(i)}) = \beta \cdot \left(\phi(s_h^{(i)}, a_h^{(i)})^T \Lambda_h^{-1} \phi(s_h^{(i)}, a_h^{(i)}) \right)^{\frac{1}{2}}, \tag{32}$$

where β is a scaling parameter. With this uncertainty penalty, PEVI can eliminate spurious correlations from the suboptimality (equation 2) and achieve mini-max optimal in linear MDPs. We then proof the uncertainty used in SCORE is equivalent to equation 32.

Suppose we use the Gaussian prior to initialize the parameters, i.e., $\widehat{w}_h \sim \mathcal{N}(0, \mathrm{I}/\lambda)$, we assume there is an approximation error ϵ when fitting the dataset $\mathcal{D}$ with the parameter $\widehat{w}_h$, i.e., $y^{(i)} = \widehat{w}_h^T \phi(s_h^{(i)}, a_h^{(i)}) + \epsilon$ where $\epsilon \sim \mathcal{N}(0, 1)$. As a result, we have:

$$y^{(i)} \sim \mathcal{N}(\widehat{w}_h^T \phi(s_h^{(i)}, a_h^{(i)}), 1). \tag{33}$$

Now we use the Bayes rule to derive the posterior of the parameter w:

$$\begin{aligned} \log p(\widehat{w}_h|\mathcal{D}) &= \log p(\widehat{w}_h) + \log p(\mathcal{D}|\widehat{w}_h) + C \\ &= -\frac{1}{2} \widehat{w}_h^T \widehat{w}_h - \sum_{i=1}^{N} (y^{(i)} - \widehat{w}_h^T \phi(s_h^{(i)}, a_h^{(i)}))^T (y^{(i)} - \widehat{w}_h^T \phi(s_h^{(i)}, a_h^{(i)})) + C \\ &= -\frac{1}{2} (\widehat{w}_h - \mu_h)^T \Lambda_H^{-1} (\widehat{w}_h - \mu_h) + C \end{aligned} \tag{34}$$

where $\mu_h = \Lambda_h^{-1} \sum_{i=1}^{N} \phi(s_h^{(i)}, a_h^{(i)})^T y^{(i)}$ and C is a constant. The posterior distribution of the parameter $\widehat{w}_h$ is of the form:

$$p(\widehat{w}_h|\mathcal{D}) \sim \mathcal{N}(\mu_h, \Lambda_h^{-1}). \tag{35}$$

In SCORE, the bootstrapped ensemble Q networks approximates the posterior distribution of Q and we use the standard deviation of this posterior distribution to quantify the uncertainty. Taking one step further from equation 35, we derive the posterior distribution of $\widehat{Q}_h$:

$$p(\widehat{Q}_h|\mathcal{D}) \sim \mathcal{N}(\phi(s_h^{(i)}, a_h^{(i)})^T \mu_h, \ \phi(s_h^{(i)}, a_h^{(i)})^T \Lambda_h^{-1} \phi(s_h^{(i)}, a_h^{(i)})). \tag{36}$$

As a result, the standard deviation of the posterior distribution of Q can be written in the form of $\left(\phi(s_h^{(i)}, a_h^{(i)})^T \Lambda_h^{-1} \phi(s_h^{(i)}, a_h^{(i)}) \right)^{\frac{1}{2}}$, which is exactly the same as equation 32.

D Examples of The Spurious Correlation Phenomenon

In this section, we first demonstrate the spurious correlation phenomenon in the simplest Multi-Armed Bandit (MAB) setting. Then we elaborate the MDP example discussed in Section 3.1.

D.1 A Simple Example in The MAB setting

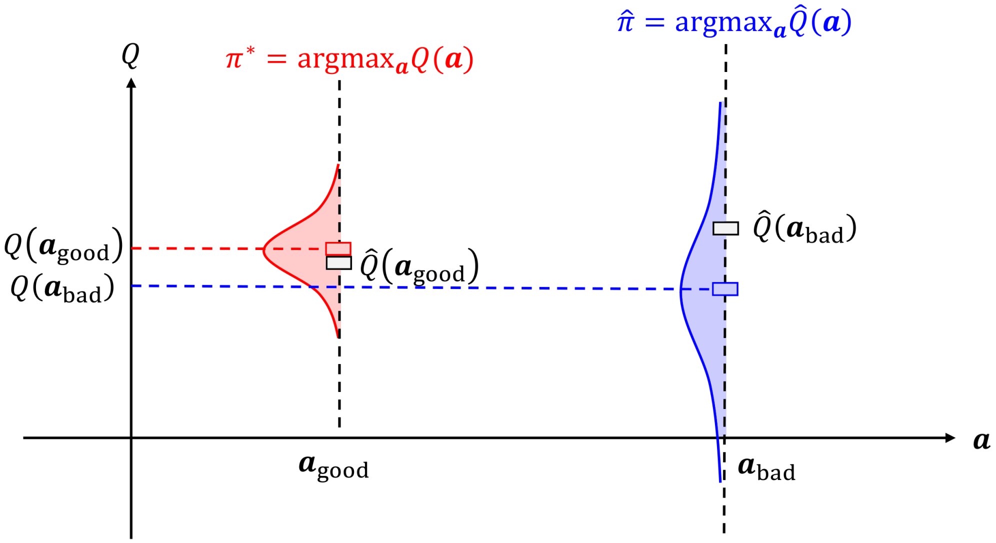
$\hat{\pi} = \text{argmax}_{\boldsymbol{a}} \hat{Q}(\boldsymbol{a})$
Q
$\pi^* = \text{argmax}_{\boldsymbol{a}} Q(\boldsymbol{a})$
$\hat{Q}(\boldsymbol{a}_{\text{bad}})$
$Q(\boldsymbol{a}_{\text{good}})$
$\hat{Q}(\boldsymbol{a}_{\text{good}})$
$Q(\boldsymbol{a}_{\text{bad}})$
$\boldsymbol{a}$
$\boldsymbol{a}_{\text{good}}$
$\boldsymbol{a}_{\text{bad}}$

Figure 6: A MAB with two actions: The reward follows a Gaussian distribution. $Q(a)$ is the expected reward of executing an action $a \in \mathcal{A}$ and $\widehat{Q}(a)$ is its sample average estimated using the dataset.

MAB is a special case of MDP, where the state space is a singleton. The agent aims to find the action maximizing the expected reward. We consider a simplified version of the example presented in Jin et al. [2021]. In our example, there are only two actions, a_{good} and a_{bad}. a_{good} has a larger expected reward so the optimal policy should always perform a_{good} rather than a_{bad}.

Consider a dataset containing a large number of a_{good} and a small number of a_{bad}. Since a_{good} has sufficient data, its sample average $\widehat{Q}$ closely match the real expected reward Q. In contrast, the sample average for a_{bad} has a large epistemic error (Equation 1). If the data of a_{bad} in the dataset by chance achieve large rewards, the sample average would overestimate the value. Figure 6 shows the real expected reward of the two actions and the sample average estimations. The optimal policy π^* chooses action a_{good} with probability one. Conversely, the greedy policy $\widehat{\pi}$ with respect to $\widehat{Q}$ takes action a_{bad}, resulting in high suboptimality (Equation 2).

D.2 Details of The Example in Section 3.1

In a general MDP that involves sequential decision-making, state transitions subtly induce spurious correlations in the offline setting. In the example discussed in Section 3.1, we consider an episodic MDP with horizon $H = 5$ as shown in Figure 7. This MDP has a deterministic reward function so there are no epistemic errors in the reward signal. For the good state s_{good}, the reward is always positive regardless of the action performed, while in the bad state s_{bad}, the agent can only get punished. Therefore, the optimal policy for this problem is to always pick the good action a_{good} to stay in/move to s_{good}.

To study the effect of spurious correlation in offline learning, we first use the optimal policy (which always executes a_{good} regardless of the state) to generate an expert dataset that contains 20 trajectories. Figure 8(a) and Figure 8(b) show the state distribution and the return distribution of the expert dataset. Since there are only two states in this MDP and the transition probabilities between states are comparable, the dataset has sufficient coverage of the entire state space. In this case, there is no state distributional shift during the evaluation process. We then make a minor modification to this dataset by adding a trajectory $\tau = [s_{\text{good}}, a_{\text{bad}}, s_{\text{good}}, a_{\text{good}}, s_{\text{good}}, a_{\text{good}}, s_{\text{good}}, a_{\text{good}}, s_{\text{good}}, a_{\text{good}}]$. Since the optimal policy never chooses a_{bad}, τ is the only trajectory that contains the transition information of executing

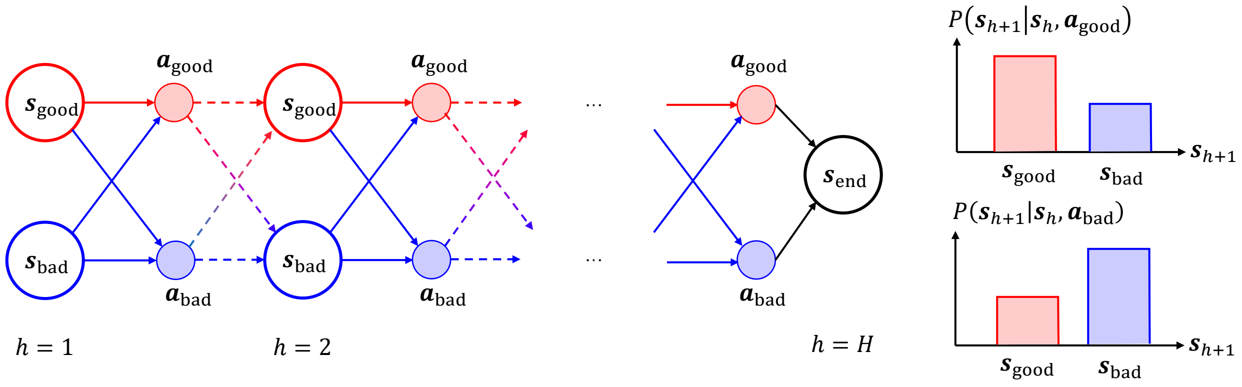

Figure 7: An episodic MDP with two states and two actions: The agent has equal probability of starting from a good state s_{good} and a bad state s_{bad}. At each step h, the agent can choose to perform either a good action a_{good} or a bad action a_{bad}. Regardless of the agent's current state s_h, the probability of transitioning into s_{good} after performing a_{good} is two-thirds, and the probability of transitioning into s_{bad} is one-third, and the opposite holds for performing a_{bad}. The reward function is deterministic and fixed for all steps, with $R(s_{\text{good}}, a_{\text{good}}) = 1$, $R(s_{\text{good}}, a_{\text{bad}}) = 0.5$, $R(s_{\text{bad}}, a_{\text{good}}) = -0.5$ and $R(s_{\text{bad}}, a_{\text{bad}}) = -1$. After H steps, the episode ends at the terminal state s_{end} and the goal is to maximize cumulative reward throughout the decision process.

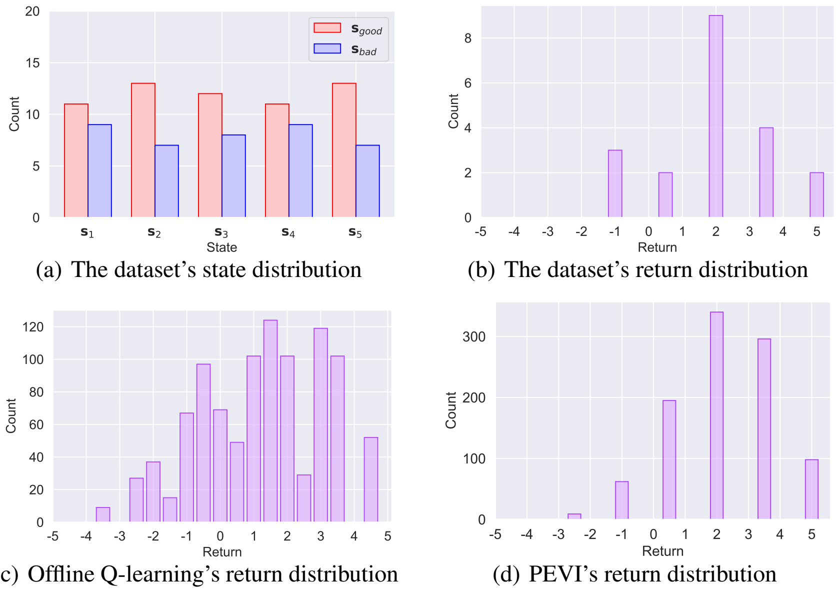

(a) The dataset's state distribution

(b) The dataset's return distribution

(c) Offline Q-learning's return distribution

(d) PEVI's return distribution

Figure 8: (a) presents the state distribution of each step $h \in [1, 5]$. s_{good} and s_{bad} have equal possbility to be the initial state. (b), (c) and (d) are the return distributions of the dataset, offline Q-learning and its pessimistic variant respectively.

a_{bad}, leading to high epistemic uncertainty. Figure 8(c) and Figure 8(d) show the return distribution of offline Q-learning and its pessimistic variant (equation 4). We remark that offline Q-learning is an offline version of the Q-learning algorithm which simply replaces the sample distribution from d^π to $\mathcal{D}$. From the return distribution we can see that offline Q-learning learns a highly suboptimal policy. The average return of this policy is much lower than in the dataset. Conversely, the pessimistic Bellman operator $\widehat{\mathcal{B}}^{-}Q(s, a)$ introduced in Section 2.2 effectively eliminate spurious correlations and perfectly recovers the optimal policy.

E Implementation Details and Additional Experiments

E.1 Experimental Settings

To guarantee a fair comparison, we conducted the experiments under the same experimental protocol. The whole training process has a total of 1 million gradient steps, which are divided into 1000 epochs. At the end of each epoch, we run 10 episodes for evaluation. To reduce the effect of randomness on the experimental results, all experiments are run with 5 independent random seeds while keeping other factors unchanged. In the end, we report the mean and standard deviation of the 5 experiments as the performance of the algorithm.

We specify both the actor network and the critic network to be a three-layer neural network with 256 neurons per layer. The first two layers of both networks use the ReLU activation function. In particular, the last layer of the actor network uses the tanh activation function for outputting actions. Both networks have a separated Adam optimizer and the learning rate is 3e-4. Some baselines differ in the settings of the network and/or the learning rate, and we follow the settings suggested by the authors in that case.

E.1.1 D4RL-MuJoCo

D4RL-MuJoCo provides five datasets of different quality for each task setting. "random" is collected using a random initialized policy, "medium" is collected using a partially trained policy, and "expert" is collected using a well-trained policy. "medium-replay" and "medium-expert" are derived from a mixture of policies [3], with the former containing all the data in the replay buffer of the "medium-level" policy and the latter being the product of mixing the "meidum" and "expert" datasets in equal proportions.

The results reported in the D4RL white paper [Fu et al., 2020] is based on the "v0" version, and most previous work reuse these results. However, the "v0" version has some errors that may lead to wrong conclusions and the authors regenerate a "v2" version. Thus, we rerun all the baseline on the "v2" version under the same protocol and report the new results.

BCQ [Fujimoto et al., 2019] is a simple yet strong baseline, providing stable performance. It involves training a Variational Auto-Encoder (VAE) and an agent with the actor-critic architecture. In particular, the actor perturbs the actions proposed by the VAE instead of directly output actions, and the critic is used to select the best action. We use the official code [4] and the suggested hyper-parameters. There are two key hyper-parameters, i.e., the max perturbation hyper-parameter Φ and the weighting for clipped double Q-learning λ, which is set to 0.05 and 0.75 respectively.

BEAR [Kumar et al., 2019] is a policy-constrained method. The behavioral policy, a VAE, is learned in the same way as BCQ. The core is the MMD constraint. We used the official implementation [5]. As suggested by the authors, the number of samples used to estimate the MMD is set to 20. We use the laplacian kernel for hopper and walker2d while halfcheetah adopts the gaussian kernel.

CQL [Kumar et al., 2020] is the state-of-the-art offline RL algorithm. Unlike policy-constrained methods, it incorporates a strong regularizer into critic's loss while the policy optimization remains unchanged. We used the official implementation [6]. The regularizer coefficient is set to 5 and the experimental results are slightly better than the results reported in the original paper.

TD3-BC [Fujimoto and Gu, 2021] is recently proposed offline reinforcement learning algorithm, which only requires minimal modifications to the TD3 [Fujimoto et al., 2018] algorithm. The author use a weighted sum of the critic loss and the behavior cloning loss to update the actor. We use the official code [7] and the suggested hyper-parameters. The weight of the critic loss is set to a constant 2.5.

MOPO [Yu et al., 2020] is a model-based offline RL algorithm which modifies the reward by incorporating the maximum standard deviation of the learned models as a penalty. We use the official implementation [8]. We roughly tune the penalty coefficient by searching in $\{0.5, 1.0, 5.0\}$ and the performance is better than using the suggested value.

[3] In practice, the behavioral policy is usually unknown and comes in the form of a mixture of multiple policies of different quality.

[4] https://github.com/sfujim/BCQ

[5] https://github.com/rail-berkeley/d4rl_evaluations/blob/master/bear

[6] https://github.com/aviralkumar2907/CQL

[7] https://github.com/sfujim/TD3_BC

[8] https://github.com/tianheyu927/mopo

Table 2: Hyper-parameters for SCORE

Hyper-parameter	Description	Value
	TD3 hyper-parameters	
σ	The std of the Gaussian exploration noise	0.2
c	The max noise.	0.5
d	The update frequency of the actor network and the target networks.	2
τ	The target network update rate.	0.005
	SCORE hyper-parameters	
M	The number of critic networks.	5
d_{bc}	The update frequency of the behavior cloning coefficient.	10000
γ_{bc}	The discount rate of the behavior cloning coefficient.	$\{0.96, 0.98, 1.0\}$
β	The uncertainty penalty coefficient.	$\{0.1, 0.2, 0.5\}$

MOReL [Kidambi et al., 2020] is also a model-based offline RL algorithm. Instead of the using the maximum standard deviation, MOReL proposes to use the maximum disagreement of the learned models as the penalty. We use the official implementation [9] and the suggested hyper-parameters. The number of models is set to 4 and the penalty coefficient is 3.0.

UWAC [Wu et al., 2021] uses MC dropout to estimate the uncertainty of the input sample and weight the loss accordingly. We use the official code [10] and the suggested setting. UWAC is based on BEAR [Kumar et al., 2019] and the hyper-parameters are kept exactly the same as in BEAR. The inverse variance is clipped to within the range of $(0.0, 1.5)$ for numerical stability. The dropout rate is 0.1.

SCORE is based on the TD3 algorithm [Fujimoto et al., 2018] and there are two main differences which correspond to the two key hyper-parameters in SCORE, i.e., the uncertainty penalty coefficient β and the discount rate γ_{bc}. We tune these two hyper-parameters on the hopper tasks, roughly searching the optimal combination in $\beta \in \{0.2, 0.5, 2.0\}$ and $\gamma_{\text{bc}} \in \{0.96, 0.98, 1.0\}$. The best combination is then used in all datasets. Empirically, we find $\beta = 0.2$ works fine on all datasets and the choice of γ_{bc} is related to the data quality. With a lower quality dataset, a smaller discount rate encourages the policy to deviate from the poor behavioral policy. For clarity, we summarize the hyper-parameters in Table 2.

E.1.2 D4RL-Adroit

There are four different tasks in D4RL-Adroit, including nail hammering, door opening, pen spinning, and ball picking/moving. Each environment consists of three types of datasets, with the "human" dataset containing only a handful of human demonstrations (25 trajectories per task). The "cloned" dataset is an equal mixture of human demonstrations and the data generated by an imitation policy. "expert" contains the data collected with a fine-tuned RL policy, which has the most samples and the best quality. Compared to MuJoCo, Adroit's tasks involve high-dimensional inputs and sparse rewards, making them extremely difficult to succeed. The narrow data distribution further increases the difficulty.

We use the newest version ("v1") of the adroit datasets in our experiments. Given that the "v1" version and the "v0" version differ only slightly in the specifications of the timeout marker and the terminal marker (the data quality is basically the same), we reuse the experimental results reported in the D4RL paper [Fu et al., 2020] which are based on the "v0" version.

UWAC [Wu et al., 2021]. Since the results of UWAC is not included in [Fu et al., 2020], we run it on the "v1" version under the same experimental protocol. The basic hyper-parameters are remained the same as in the D4RL-MuJoCo tasks. As suggested by the authors, we employ Spectral Normalization on this task suite for better stability.

SCORE. We keep most of the hyper-parameters the same as on the D4RL-MuJoCo datasets. Similar to Wu et al. [2021], we adopt Spectral Normalization in the adroit tasks.

[9] https://github.com/aravindr93/mjrl/tree/v2/projects/morel

[10] https://github.com/apple/ml-uwac

F Supplementary Experiments and Figures

F.1 Comparison Experiments on D4RL-Adroit

Table 3: Average normalized scores on the Adroit datasets. We reuse the results reported in the D4RL [Fu et al., 2020] paper. For UWAC and SCORE, we run it over 5 random seeds and report both the mean score and the standard deviation. A score of zero corresponds to the performance of the random policy and a score of 100 corresponds to the performance of the expert policy.

Task	SCORE	BC	BCQ	BEAR	UWAC	CQL	AWR	REM	αDICE
pen-human	45.2±24.1	34.4	68.9	-1.0	10.0±3.2	37.5	12.3	3.5	-3.3
hammer-human	0.2±0.0	1.5	0.5	0.3	1.2±0.7	4.4	1.2	0.2	0.3
door-human	-0.1±0.0	0.5	0.0	-0.3	0.4±0.2	9.9	0.4	-0.1	-0.0
relocate-human	-0.1±0.0	0.0	-0.1	-0.3	0.0±0.0	0.2	0.0	-0.2	-0.1
pen-cloned	31.2±12.7	56.9	44.0	26.5	23.0±6.9	39.2	28.0	-3.4	-2.9
hammer-cloned	10.5±15.6	0.8	0.4	0.3	0.4±0.0	2.1	0.4	0.2	0.3
door-cloned	0.0±0.0	-0.1	0.0	-0.1	0.0±0.0	0.4	0.0	-0.1	0.0
relocate-cloned	0.0±0.0	-0.1	-0.3	-0.3	0.0±0.0	-0.1	-0.2	-0.2	-0.3
pen-expert	121.4±21.2	85.1	114.9	105.9	98.2±9.1	107.0	111.0	0.3	-3.5
hammer-expert	130.3±0.4	125.6	107.2	127.3	107.7±21.7	86.7	39.0	0.2	0.3
door-expert	105.6±1.9	34.9	99.0	103.4	104.7±0.4	101.5	102.9	-0.2	0.0
relocate-expert	97.9±12.4	101.3	41.6	98.6	105.5±3.2	95.0	91.5	-0.1	-0.1
Overall	**45.2±7.3**	36.7	39.7	38.41	37.6±3.8	40.31	32.2	0.0	-0.8

The experimental results are presented in Table 3. As discussed in Fu et al. [2020], the adroit datasets have very narrow distributions and the data quality is highly unstable. These factors, along with high-dimensional inputs and sparse rewards, pose huge challenges to existing offline RL algorithms. We can see that most algorithms fail completely in both the human and cloned settings, including SCORE. This motivates us to further investigate the techniques required to overcome the above challenges in future work. Nevertheless, SCORE works well on the expert dataset and has the highest overall performance.

F.2 Hyper-parameter Analyzes

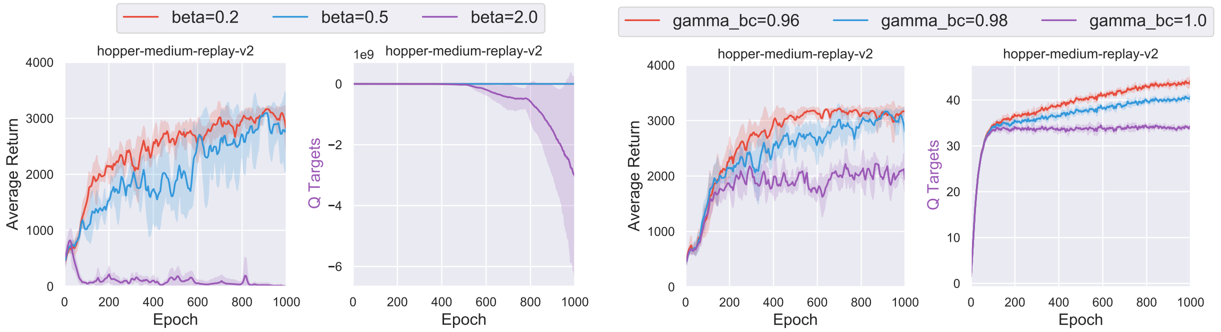

(a) (b)

Figure 9: (a) shows the average return and the Q target of SCORE with different β. (b) shows the average return and the Q target of SCORE with different γ_{bc}

F.2.1 The Uncertainty Penalty Coefficient

The uncertainty penalty coefficient β controls the degree of pessimism. We conduct experiments by choosing β from $\{0.2, 0.5, 2.0\}$. The experimental results are shown in Figure 9(a). We can see that $\beta = 0.2$ and $\beta = 0.5$ works similarly on this dataset while $\beta = 2.0$ results in over-pessimistic Q values. When the penalty is too large, the agent tends to act conservatively and fails to fully exploit the dataset, which lead to poor performance.

F.2.2 The Discount Rate of Behavior Cloning

We use a decaying factor γ_{bc} to control the weight of the behavior cloning loss in policy's objective function. We choose discount rate γ_{bc} from $\{0.96, 0.98, 1.0\}$ to validate the sensitivity with respect to behavior cloning. We remark that $\gamma_{\text{bc}} = 1$ corresponds to a constant weight. From Figure 9(b) we can see that $\gamma_{\text{bc}} = 0.96$ and $\gamma_{\text{bc}} = 0.98$ work similarly in this dataset, with $\gamma_{\text{bc}} = 0.96$ converges faster. In contrast, $\gamma_{\text{bc}} = 1.0$ results in a sub-optimal policy that converges prematurely. This is because the medium-replay dataset is generated by a mixture of policies of different quality. A strong behavior cloning regularizer hinders the agent to take the essence and discard the dross. Overall, when the dataset is of low or medium quality, a smaller γ_{bc} is more preferable.

F.3 Figures

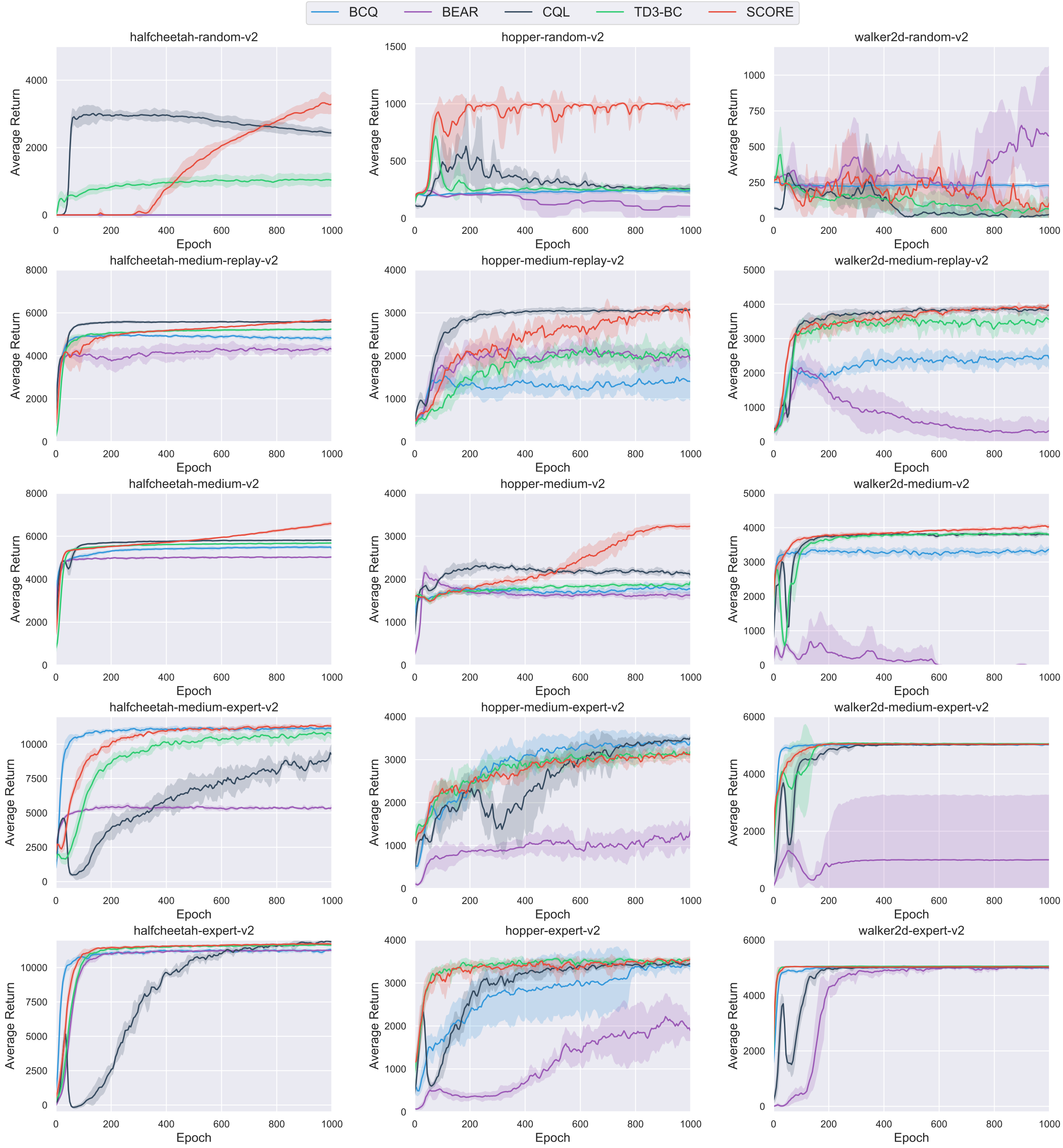

Figure 10: The average return of SCORE and the baseline methods throughout the training process. Overall, the performance of SCORE improves with data quality, which is consistent with the theoretical results in Jin et al. [2021], i.e., the upper bound of suboptimality depends only on how well the dataset covers the state-action distribution of the optimal policy, not the entire state-action space.

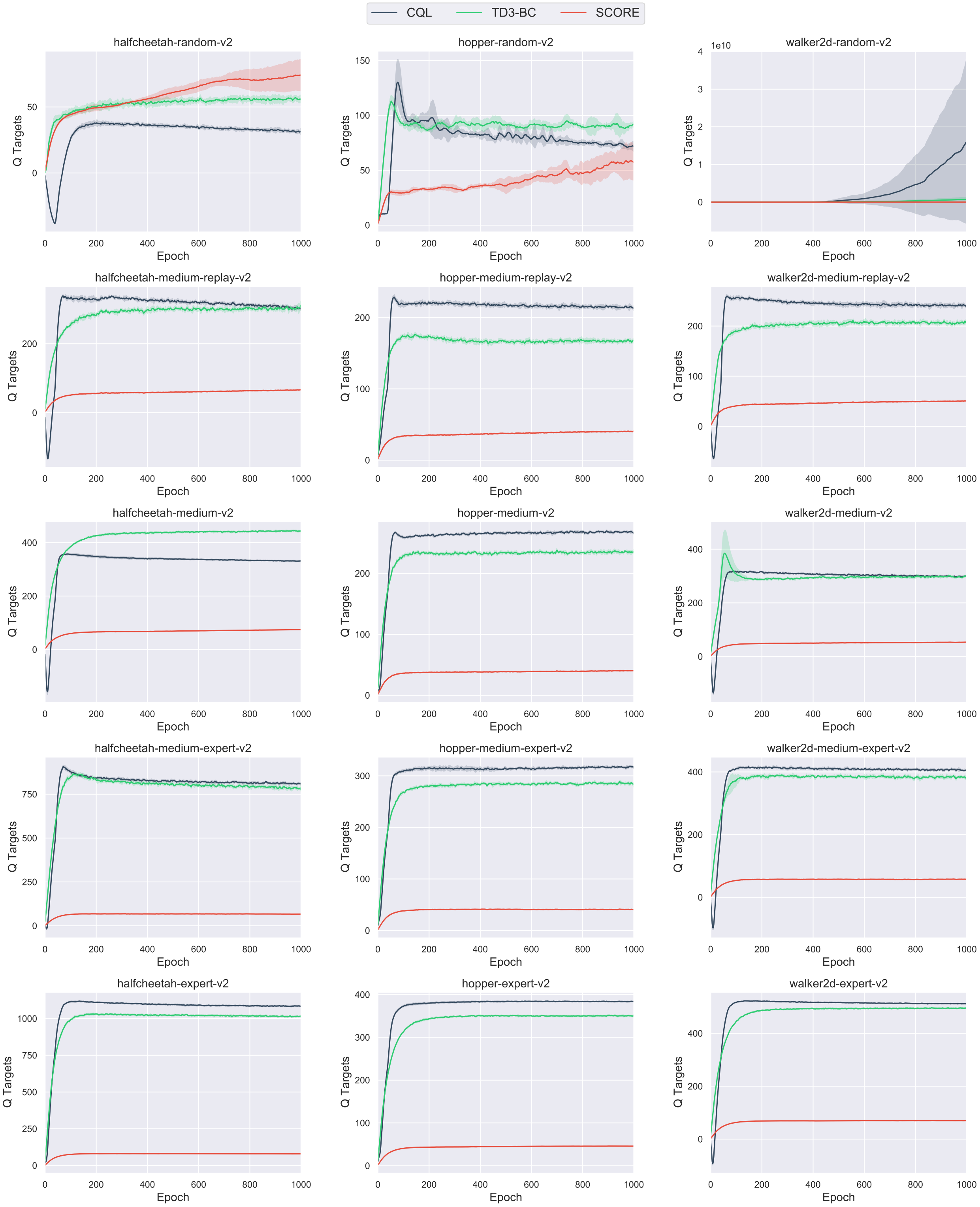

Figure 11: The mean value of Q targets of SCORE, TD3-BC and CQL throughout the training process. TD3-BC and CQL perform the best amongst all baselines. All three methods provide stable estimations of the Q value without explosions or large oscillations.